Science of the Total Environment

Life in plastic, it's not fantastic: Sublethal effects of polyethylene microplastics ingestion throughout amphibian metamorphosis

Running title: Sublethal effects of microplastics on amphibians

Katharina Ruthsatz[1], Anja Schwarz[2], Ivan Gomez-Mestre[3], Ruth Meyer[2], Marie Domscheit[1], Fabian Bartels[1], Sarah-Maria Schaeffer[2], Karolin Engelkes[4,5]

[1]*Zoological Institute, Technische Universität Braunschweig, Mendelssohnstraße 4, 38106 Braunschweig, Germany*

[2]*Institute of Geosystems and Bioindication, Technische Universität Braunschweig, Langer Kamp 19c, 38106 Braunschweig, Germany*

[3]*Ecology, Evolution, and Development Group, Department Ecology and Evolution, Doñana Biological Station, CSIC, 41092 Seville, Spain*

[4]*Leibniz Institute for the Analysis of Biodiversity Change, Martin-Luther-King-Platz 3, 20146 Hamburg, Germany*

[5]*Institute of Evolutionary Biology and Ecology, University of Bonn, An der Immenburg 1, 53121 Bonn, Germany*

Corresponding author: **Katharina Ruthsatz**; ORCID: 0000-0002-3273-2826. Current address: Zoological Institute, Technische Universität Braunschweig, Mendelssohnstraße 4, 38106 Braunschweig, Germany. Phone: 0049 531 3912393. Email: katharinaruthsatz@gmail.com.

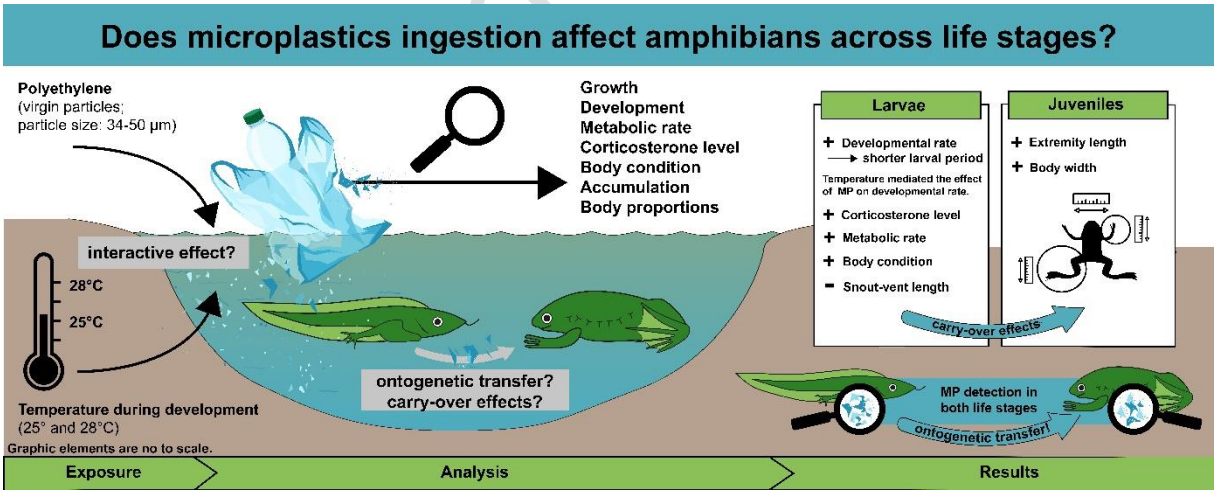

Abstract

Microplastics (MP) are an abundant, long-lasting, and widespread type of environmental pollution that is of increasing concern as it might pose a serious threat to ecosystems and species. However, these threats are still largely unknown for amphibians. Here, we used the African clawed frog (*Xenopus laevis*) as a model species to investigate whether polyethylene MP ingestion affects amphibian growth and development and leads to metabolic changes across two consecutive life stages (larvae and juveniles). Furthermore, we examined whether MP effects were more pronounced at higher rearing temperatures. Larval growth, development, and body condition were recorded, and standard metabolic rate (SMR) and levels of stress hormone (corticosterone, CORT) were measured. We determined variation in size, morphology, and hepatosomatic index in juveniles to identify any potential consequences of MP ingestion across metamorphosis. In both life stages, MP accumulation in the body was assessed. MP ingestion was found to result in sublethal effects on larval growth, development, and metabolism, to lead to allometric carry-over effects on juvenile morphology, and to accumulate in the specimens at both life stages. In larvae, SMR and developmental rate increased in response to MP ingestion; there additionally was a significant interaction of MP ingestion and temperature on development. CORT levels were higher in larvae that ingested MP, except at higher temperature. In juveniles, body was wider, and extremities were longer in animals exposed to MP during the larval stage; a high rearing temperature in combination with MP ingestion counteracted this effect. Our results provide first insights into the effects of MP on amphibians throughout metamorphosis and demonstrate that juvenile amphibians may act as a pathway for MP from freshwater to terrestrial environments. To allow for generalizations across amphibian species, future experiments need to consider the field prevalence and abundance of different MP in amphibians at various life stages.

Key words

carry-over effects, plastics accumulation, ontogenetic transfer, standard metabolic rate, environmental stress, Xenopus laevis

1. Introduction

Environmental pollution poses a serious threat to wildlife and ecosystem health and is in part responsible for the ongoing biodiversity loss associated with anthropogenic global change (Wake and Vredenburg, 2008; Noyes and Lema, 2015; da Silva et al., 2018). Today, one of the fastest-growing sources of pollution are microplastics (MP) (Borrelle et al., 2017; Akdogan and Guven, 2019) due to the global increase in plastic consumption and a poor management in plastic waste (Li et al., 2018; PlasticsEurope, 2022). MP are defined as synthetic polymer particles between 1 µm and 5 mmin diameter (particles <1 µm are defined as nanoplastics; Thompson, 2004; Hartmann et al., 2019) which derive either from primary (i.e., medicines, personal care products, pellets for plastic production, and textiles (Horton et al., 2017), or secondary plastics (i.e., debris of plastic items, fishing nets, and tires; Horton et al., 2017) that differ in size, shape, chemical composition, and texture (Hale et al., 2020; Bhattacharya and Khare, 2022). Considering their size range, MP might be an ideal prey item for a variety of aquatic animals, including zooplankton, molluscs, hexapods, crustaceans, fish, and amphibians, and are thus, available for ingestion (Franzellitti et al., 2019). MP ingestion can trigger a variety of harmful effects on digestive, endocrine, and nervous systems which might ultimately impair development, growth, physiology, reproduction, and survival (rev. in Prokić et al., 2019). Additionally, MP can be accumulated and transferred through the food chain (Diepens and Koelmans, 2018) and particles might serve as a biological or chemical vector for organisms and pollutants (Hartmann et al., 2017) or can even carry pathogens (Kirstein et al., 2016). Considering that amphibian population declines are at the forefront of the biodiversity crisis (Stuart et al., 2004; IUCN, 2022), understanding the ecotoxicological risks posed by MP to amphibians is highly relevant for their conservation.

Amphibians often have a complex, biphasic life cycle with aquatic and terrestrial stages (Gomez-Mestre et al., 2012) and play a key role in the food web (Hocking and Babbitt, 2014). Consequently, amphibians might potentially transfer contaminants like MP across trophic levels and from freshwater to terrestrial ecosystems, and *vice versa* (Pastorino et al., 2022). In contrast to other aquatic vertebrates, however, data on the capacity to accumulate MP are limited in amphibians (Prokić et al., 2021; Pastorino et al., 2022) and no study so far has assessed possible ontogenetic transfer pathways within their complex life cycle. Similarly, the research on the (sublethal) effects of MP ingestion in amphibians is still limited (rev. in Burgos-Aceves et al., 2022). Recent studies on amphibian larvae demonstrated that MP ingestion leads to alterations of anti-predatory behavior (da Costa Araújo and Malafaia, 2020), growth (Balestrieri et al., 2022), body condition (Boyero et al., 2020), developmental rate and intestinal morphology (Ruthsatz et al., 2022a). It also causes MP accumulation in the digestive tract (Hu et al., 2016), increases susceptibility to pathogens (Bosch et al., 2021), and causes histopathological transformations of the liver through cytotoxicity (da Costa Araújo et al., 2020a, 2020b). As the gut is the functional link between energy intake and energy allocation (Ruthsatz et al., 2022a, 2019), disruptions of its normal function may result in adverse effects on food intake and/or nutrient absorption, causing metabolic changes with consequences for growth, development, immune function, energy budget, and ultimately survival. In contrast to fish and aquatic invertebrates (Franzellitti et al., 2019), such toxicological effects of MP ingestion and accumulation on the metabolic health are largely unknown in amphibians, and longitudinal studies across life stages are completely missing.

In global change reality, amphibians often have to simultaneously cope with stressors of natural and anthropogenic origin. These environmental stressors can interact with the effects of MP, and elicit either synergistic, neutral, or antagonistic effects on organisms (Castro-Castellon et al., 2021). As amphibians are ectotherms, thermal stress is a determinant environmental stressor and arguably the most important in the face of climate change. Several studies suggest that

environmental stressors associated with climate change including desiccation and temperature variation could increase the effects of aquatic pollutants such as MP on amphibians (e.g., Rohr et al., 2011; Curtis and Bidart, 2021). Alternatively, pollutants are thought to reduce the tolerance of amphibians to rising temperatures (Ruthsatz et al., 2020a) or affect the immune system of (larval) amphibians, making them more susceptible to infections (Bosch et al., 2021). A recent study found that experimental warming reduced the effect of MP on metabolic rate in the freshwater amphipod *Gammarus pulex* (Kratina et al., 2019). In contrast, Reichert et al. (2021) could only find minor and infrequent cumulative negative effects of MP with that of global warming on reef-building coral species. In order to realistically predict the consequences of MP pollution on amphibian populations, it is of key importance to assess whether the combined exposure to environmental stress and MP pollution incurs synergistic effects on amphibian growth, development, and metabolism, and whether these effects are carried throughout their life cycle.

Here, we investigated whether MP ingestion (polyethylene, particle size: 34-50 µm) affects growth and development in amphibian larvae, and whether it causes metabolic changes across two consecutive life stages using the African clawed frog (*Xenopus laevis*) as a model species. Furthermore, we also examined whether MP effects could be exacerbated at higher rearing temperatures. In larval *X. laevis*, development and growth, body condition as well as corticosterone (CORT) level, and standard metabolic rate (SMR) were measured. After metamorphosis, juvenile size (body mass and snout-vent-length (SVL), as well as morphology (fore- and hindlimb length, body width) were recorded. Furthermore, the hepatosomatic index (HSI) was calculated to assess possible carry-over effects of MP ingestion on energy reserves throughout metamorphosis. In both life stages, MP accumulation in the body was assessed. This study will provide first insights into the complex (sublethal) effects of MP on amphibians across life stages and will allow us to estimate the potential of amphibians to transfer MP from freshwater to terrestrial ecosystems by unveiling the capacity for an ontogenetic transfer of MP.

2. Material & Methods

2.1 Study species

As a model organism, we chose the amphibian *Xenopus laevis*, a thoroughly studied amphibian with regards to its growth, development, and physiology as a model organism (Buchholz, 2017). Given that they are filter-feeders, *Xenopus* tadpoles provide an excellent model for studying the effects of MP consumption in repeatable tests with dispersed particles. Recently, both *Xenopus* embryos and larvae have been used for investigating the ecotoxicology of MP in amphibians under controlled laboratory conditions (rev. in Hu et al., 2016; Bacchetta et al., 2021; Venâncio et al., 2022; Ruthsatz et al., 2022a).

2.2 Experimental design and animal culture

A two-phase experimental design was chosen to assess the effects of MP ingestion during larval development on larvae (phase 1; developmental stage NF57 according to Nieuwkoop and Faber, 1994) and juveniles (phase 2; 10 days after completing metamorphosis = NF 66 + 10 days). The experiment was conducted in a climate chamber (Kälte-Klimatechnik-Frauenstein GmbH, Germany) with a 14:10 h light:dark cycle and a mean (± SD) air temperature of 20 (± 0.2) °C in November and December of 2021. Three treatments – control, MP, and cellulose fibers – and two temperatures – 25 °C and 28 °C – were utilized in a 3 x 2 experimental setup, and each treatment had three replicates. (i.e., aquaria; 18 aquaria in total). The experiments ran for 7 weeks.

Phase 1. – Five clutches (i.e., full-sib families) of *X. laevis* eggs were provided by the Universitätsklinikum Hamburg Eppendorf. Until the embryos hatched and reached

developmental stage NF45 (i.e., when exotrophic feeding occurs), each clutch was kept separately at 22 °C in a bucket filled with aged de-chlorinated water. Then, three larvae from each clutch were randomly allocated to each of the 18 standard 12-L aquaria filled with 9 L of aged de-chlorinated water. Each aquarium housed 15 larvae (15 larvae × 18 aquaria = 270 larvae in total; larval density: 1.66 larvae × $L^{-1)}$. Nine of the aquaria were kept at a mean (± SD) water temperature of 25 (± 0.1) °C, the other nine at 28 (± 0.3) °C by using adjustable heating elements (JBL PROTEMP S 25, 25 W, JBL GmbH & Co. KG, Germany). Three aquaria (i.e., replicates) of each temperature treatment were exposed to the MP treatment, other three to the natural fiber control group (i.e., cellulose), and the remaining three were used as control group without fiber exposure (3 replicates × 3 treatments × 2 rearing temperatures = 18 aquaria in total). Larvae were fed high-protein powdered fish food (Sera micron, Sera, Germany). To guarantee that food was available in abundance, *ad libitum* rations were provided. Dead tadpoles were removed from the aquaria.

Phase 2. – After completing metamorphosis (developmental stage NF66), all surviving animals remained in their phase 1 aquaria at the same rearing temperatures as during phase 1. Froglets were fed *ad libitum* with high-protein frog food granules (Tetra ReptoFrog Granules, Tetra GmbH, Germany). Exposure to MP and cellulose fibers was stopped after completion of metamorphosis. Final measurements were taken ten days after the completion of metamorphosis. Animals that were not subjected to the final measurements remained at the institute.

Both food types were free of MP (see section 2.7; Fig. S1). Particle size of food provided to the larvae during experimental phase 1 was in the range of MP and cellulose particle size (Fig. S1).

2.3 Particle and fiber exposure

In the experiment, polyethylene MP particles (Sigma-Aldrich; polyethylene powder, CAS number 9002-88-4, particle size: 34-50 µm, density 0.94 g/mL) was used. As one of the most widely utilized polymers to produce plastic materials (Horton et al., 2017), polyethylene has been identified as an environmentally relevant MP pollutant in amphibians (Karaoğlu and Gül, 2020) and has been consequently used in studies testing the effect of MP on amphibian behavior and health (da Costa Araújo et al., 2020a, 2020b, Ruthsatz et al., 2022a). Following the procedure of da Costa Araújo et al. (2020a), a MP concentration of 60 mg/L was applied to be comparable with this study. The chosen MP concentration corresponds to 1.0356-1.0675 x 10^7 particles per liter (see Supplementary Material for details on particle count determination). The selected concentration is environmentally relevant as it is within the range of surface water contamination with MP (Koelmans et al., 2019) but represents a highly polluted freshwater ecosystem (da Costa Araújo et al., 2023, 2020a). According to Anbumani and Kakkar (2018), MP concentrations found in surface water can vary and might be lower than the ones often tested under laboratory condition (Hu et al., 2022: 1.27 ± 0.306–6.73 ± 3.23 items/L; Schrank et al., 2022: 0.7 to 354.9 particles/m^3; Olesen et al., 2019: 270 particles/L; but not: Rehse et al., 2016: 400 mg/L; rev. in da Costa Araújo et al., 2020b).

Since natural systems contain a wide range of naturally occurring non-digestible particles similar in size and shape to MP particles (Buss et al., 2021), cellulose (Sigma-Aldrich; cellulose powder, CAS number 9004-34-6, particle size: 51 µm) was included as a natural fiber control group in our experimental design. The cellulose concentration was similar to the concentration used for the MP treatment (i.e., 60 mg × L^{-1}). Both MP and cellulose were directly added to the aquaria (i.e., 60 mg × L^{-1} × 9 L water = 540 mg particles per aquarium; see Supplementary Material for details). Wooden-made air stones guaranteed aeration of the water as well as continuous dispersion of fibers within the water avoiding article settlement or the formation of an MP film on the water surface (Ruthsatz et al., 2022a).

Every second day, water was changed completely following the procedure outlined in Ruthsatz et al. (2022a). Wastewater was filtered in order to remove MP particles before disposal. To avoid any MP contamination in the experimental climatic chamber, only cotton-made tissues and clothes were used. Moreover, we used an air purifying system (Philips AC2889/10, CADR 333$m^3 \times h^{-1}$) to filter possible air contamination of MP (Ruthsatz et al., 2022a).

2.4 Life history variables, ontogenetic staging, and survival

Snout-vent length and body mass were measured at three experimental points: before the start of the experiment (i.e., directly after hatching), at the end of experimental phase 1 (i.e., developmental stage NF57) as well as at the end of the experiment (i.e., ten days after completing metamorphosis). The SVL of the animals was measured with a digital caliper to the nearest 0.5 mm. To assess the body mass, we dry blotted and weighed the specimens to the nearest 0.001 g with an electronic balance (Sartorius A200 S, Germany). Duration of larval period was quantified in days after hatching (dah). Every other day, we determined ontogenetic stage by assessing the status of key morphological features as detailed in Nieuwkoop and Faber (1994). According to Ruthsatz et al. (2020a), larval growth rate (mg per day after hatching; GR) was calculated from mass at the stage NF57 minus the mass directly after hatching, divided by the days from hatching to reaching stage NF57 (i.e., 'age'). Mortality was low across all treatments throughout the experiment (4.07 %, N = 11) and was therefore not statistically analyzed.

2.5 Physiological measurements in larvae

When larvae reached developmental stage NF57 (i.e., all five toes separated), specimens were randomly selected from each aquarium (90 larvae in total) for SMR measurements. Thereafter, 54 of these larvae (three per replicate/aquarium) were sacrificed and frozen at -80 °C. All other larvae were transferred back to their respective aquaria. Body condition was calculated for all 90 larvae, see below.

2.5.1 Metabolism measurements

Closed respirometry was applied to quantify oxygen consumption between 0900 and 2100h during the natural activity phase at the respective rearing temperature (25 °C or 28 °C). Collected animals were not fed 24 h prior to and during the SMR measurements and therefore, were in a post-absorptive state (Orlofske et al., 2017). In order to exclude microbial oxygen consumption, larvae were measured in 30-mL glass vessels (i.e., respiration chambers) filled with autoclaved tap water. In each respiration chamber, a chemical optical oxygen sensor spot was integrated, which was connected to a multichannel oxygen measuring system (Oxy-4 SMA; PreSens Precision Sensing GmbH, Regensburg, Germany) via a fiber optic sensor (Polymer Optical Fiber POF, PreSens Precision Sensing GmbH, Regensburg, Germany). Respiration chambers were sealed with airtight rubber plugs. A temperature probe submerged in the water bath with the chambers (i.e., at the same temperature) provided temperature compensation for dissolved oxygen measurements. The O_2 fiber optic sensors were calibrated with air-saturated water and a factory-set zero oxygen calibration point at the respective rearing temperature prior to each trial.

To prevent recording effects of handling stress, O_2 concentration was measured after a 10-minute acclimation interval following the introduction of animals into the respiration chambers. In the beginning, the water was at 100 % O_2 saturation. For 20 min, the O_2 concentration was recorded every 15 seconds and measured as mL $O_2 \times L^{-1}$ (volume not corrected for the size of the animal). To minimize acute handling effects, readings recorded in the first five minutes of each experiment were disregarded. In every trial, empty (control) chambers were run

simultaneously, and values were adjusted accordingly. To prevent respiration from being impeded at low O_2 saturation levels, we ensured that less than 10 % of total O_2 was removed during each trial. At the end of the oxygen consumption measurements, 54 larvae were assigned to CORT level measurements. Dry blotted body mass and SVL were determined for all remaining larvae, which were then returned to the respective aquaria.

2.5.1.1 Standard metabolic rate calculations

The analyses were performed using PreSens Oxygen Calculator Software (PreSens Precision Sensing GmbH, Regensburg, Germany) as described in Ruthsatz et al. (2022b). First, O_2 consumption of each animal was plotted over time over time and visually evaluated activity peaks to omit them from the SMR calculation (Peck and Moyano, 2016). SMR was expressed in mL $O_2 \times h^{-1} \times g^{-1}$ wet body mass and was determined from the slope of linear least squares regression of O_2 concentration *vs*. time (Hastings and Burggren, 1995).

2.5.2 Corticosterone (CORT) assay

Larvae were anaesthetized in 2 g × L^{-1} tricaine methanesulfonate (MS-222, Ethyl 3-aminobenzoate methanesulfonate; Sigma-Aldrich), dissolved in buffered ultrapure water (Ramlochansingh et al., 2014) until they did not respond to external stimuli. Although MS-222 may affect CORT levels (e.g., Smith et al., 2018; Hernández et al., 2012; Archard and Goldsmith, 2010), this should not impair our results as all animals were handled the same way and processed in under 3 min (Mausbach et al., 2022). We then quickly determined dry blotted body mass and SVL in each larva. The tail was cut and placed in a sterile 1.5 mL tube and then snap frozen in liquid nitrogen for CORT analyses. Until extraction, samples were stored at -80 °C.

Tissue CORT samples were shipped overnight on dry ice to Doñana Biological Station in Seville, Spain. Extraction took place in October of 2022. For extraction, samples were randomly thawed, weighed to the nearest 0.00001 g and individually homogenized in 16 × 100 mm glass tubes with 500 µL PBS buffer (AppliChem Panreac, Germany) using a homogenizer at ~ 17,000 rpm (Miccra D-1, Germany). The tissue blender was washed into the tube with additional 500 µL PBS buffer, in order to collect the sample residue. Then, it was cleaned with ddH_2O, and 96 % EtOH between samples. After homogenization, 4 mL of a 30 %:70 % petroleum ether:diethylether dissolvent mixture (both from Sigma-Aldrich, Germany) was added to each sample. The samples were vortexed for 60 s and subsequently centrifuged at 1,800 g and 4 ºC for 15 min. After centrifugation, samples were snap frozen in a dry ice ethanol bath for 5 min. The resulting top organic fraction containing CORT was poured into a new 16 × 100 mm glass tube. All steps after homogenization were then repeated to ensure maximum CORT extraction. Both ether fractions of each sample were then pooled into a single tube and thereafter evaporated in a sample concentrator (Techne FSC400D; Barloworld Scientific, United Kingdom) using a constant but gentle nitrogen flow. Lipids were then resuspended in 315 µL EIA buffer using vortex, and incubated overnight at 4 °C.

Corticosterone levels were measured using DetectX Corticosterone ELISA (Enzyme Immunoassay) kits (Arbor Assays, K014-H5, Ann Arbor, MI, USA). Before plating, samples and kit reagents were brought to room temperature and vortexed. The 100 µL assay format for standard preparations and assays was used. Corticosterone concentration was measured in triplicates for all samples on 96-well plates. The plates were read with a multimode microplate reader (Victor 3, PerkinElmer; in Seville) at 450 nm. In total, 4 plates were run.

MyAssays online tools was used to calculate the hormonal concentration of samples (https://www.myassays.com/arbor-assays-corticosterone-enzyme-immunoassay-kit-improved-sensitivity.assay). All the measurements of triplicates with a coefficient of variation lower than

or equal to 30 % or with an absolute difference between mean and median lower than 2.5 pg were kept. For the samples that did not meet those requirements, we discarded the most different value of the triplicate. Standards run on each plate were utilized to calculate intra- and interplate coefficient of variation (Ruthsatz et al., 2023). Our analysis yielded an inter-assay variation of 18.52 % and an intra-assay variation of 20.49 %. The mean coefficient of variation of triplicates for all samples was 12.97 %. Average R^2 for the 4PLC fitting curve was 0.99. Each ELISA plate also included a negative control. Hormone samples were adjusted for the average background corticosterone measured in negative control samples. CORT levels were expressed in pg × mg^{-1}.

2.5.3 Body condition

Following Peig and Green (2010, 2009), body condition was determined using the scaled mass index (SMI). The SMI is calculated from the regression of log transformed SVL and log transformed mass (Peig and Green, 20010, 2009; Ruthsatz et al., 2020b, 2018):

$$\text{SMI} = \left[individual\ Mass \times \left(\frac{mean\ SVL\ of\ population}{individual\ SVL}\right)^{slope\ of\ regression\ logMass\sim logSVL}\right]$$

2.6 Morphological and physiological measurements in juveniles

At the end of the experiment (i.e., ten days after completing metamorphosis at NF66), four juveniles were randomly selected from each aquarium (12 specimens per treatment, 72 specimens in total). The collected animals were immediately euthanized with 6 g × L^{-1} of tricaine methanesulfonate (MS-222, Ethyl 3-aminobenzoate methanesulfonate; Sigma-Aldrich) and washed with filtered water in order to remove external fibers. Then, specimens were preserved in an increasing ethanol series (30 % for 24 h, 50 % for 24 h, and 70 % for 7 d) for morphometric measurements (N = 72) and liver and gut dissections (N = 36; sub-sample).

2.6.1 Morphometric measurements

The lengths of the forelimbs and the segments of the hindlimbs (i.e., femur, tibiofibula length, and foot length; Table S1) were measured in dorsal view to the nearest 0.001 mm using a Keyence VHX-500F digital microscope. To avoid any potential bias, the treatments were renamed with the names of arbitrary cities prior to measurement acquisition such that the observer who took the measurements (MD) did not know to which treatment a given specimen belonged. Each specimen was placed into a new, clean petri dish for measuring and all specimens of a given treatment were measured in a row after the bench and tools had been thoroughly cleaned to preclude the contamination of specimens with particles they were not exposed to during the experiment.

The precision of the measurements was assessed measuring the morphological variables six times in one specimen per treatment (6 specimens in total; maximum relative standard deviation: 0.72). The specimens used for the assessment were included in the subsequent analyses using the mean values of the measurements for each specimen. All measured limb dimensions were size-corrected by performing separate linear regressions of log10-transformed limb dimension on the log10-transformed SVL. In addition, the tibiofibula-to-femur ratio was calculated by dividing the tibiofibula length by the femur length. The residuals of the regressions and the tibiofibula-to-femur ratios were used in the statistical analyses.

2.6.2 Liver dissections and hepatosomatic index

We dissected the livers and guts of a sub-sample of 36 out of the 72 juvenile frogs used for morphometric measurements using a digital microscope (Keyence VHX-500F). Livers were dabbed and weighed to the nearest 0.001 g with an electronic balance (Sartorius A200 S,

Germany). Dissected livers and animal remains were stored in ethanol (70 %). Dissected guts were stored individually. All parts of the sub-sample were then proceeded to subsequent accumulation analyses; the gut was analyzed separately from the remaining parts of each specimen.

We estimated size of energy stores in juvenile *X. laevis* by calculating the hepatosomatic index (HSI; Htun-Han, 1978; Jelodar and Fazli, 2012; Ruthsatz et al., 2018), a condition index that describes the status of energy stored in the liver of animals and can therefore be used for estimating the recent fat storage in animals (Htun-Han, 1978; Bolger and Connolly, 1989). A decline in HSI shows that liver fat reserves are mobilized to meet metabolic requirements (Jelodar and Fazli, 2012). The HSI was calculated according to the method of Htun-Han (1978):

$$\boldsymbol{HSI = \frac{\text{liver wet weight}}{\text{whole body wet weight}}\ x\ 100}$$

2.7 MP accumulation before and after metamorphosis

One larva of each aquarium was randomly selected at the end of phase 1, euthanized, washed with filtered water, and preserved as above. The juvenile specimens (N = 72) used for morphometric measurements and liver dissection (i.e., the sub-sample of these frogs) were used for MP accumulation assessment after metamorphosis.

To examine whether MP accumulated in the larvae and to assess a possible transfer of accumulated MP across the metamorphic boundary in juvenile frogs, all samples (i.e., total larvae, total juveniles, juvenile remnant bodies and juvenile guts) were dissolved using various reagents. For this purpose, the complete bodies (larvae and juvenile frogs, all double encoded), which were kept refrigerated in ethanol, were first washed thoroughly again, blotted dry and weighed to the nearest 0.001 g (KERN EW 420-3NM, Germany). After transferring the bodies or their remnants (juvenile frog guts, juvenile remnant bodies including the livers) into 100 mL Erlenmeyer flasks, 8 mL H_2O_2 and 3 mL concentrated HCl were added to each. The flasks were then heated for 30 min at 50-65 °C in a water bath, with a controlled increase in temperature. This was followed by centrifugation twice at 4200 rpm for 10 min and subsequent washing. The residues were then mixed with 10 mL of concentrated H_2SO_4, transferred back to the flasks, and 1 mL of concentrated $KMnO_4$ solution was added to each. After boiling the suspensions again for 10 min at 60 °C in a water bath, saturated oxalic acid was added dropwise until the suspensions cleared. This was followed by repeated washing until the reaction was neutral. The suspensions were dropped completely onto 1-2 coverslips, dried overnight, and then permanently embedded in Naphrax (n = 1.71) on slides.

Afterwards, light microscopic analysis to determine MP in the prepared slides were performed on an Axio Imager.M2 (Zeiss, Germany) research microscope at 400x magnification using differential interference contrast. Particle counts were divided by animal body mass (i.e., mass obtained directly before the dissolution process) to achieve relative values comparable across specimens and live stages.

Following the same procedure as described for the larval and juvenile bodies, both food types as well as the Cellulose powder were checked for MP particles (N = 4 per sample type).

2.8 Statistics

For all statistical tests Cran R (Version 4.1.1, R Development Core Team 2021) for Windows was used unless otherwise noted. All plots were constructed using ggplot2 (Wickham, 2009) and Adobe Illustrator CS6. For all tests and models, statistical significance was set at $\alpha < 0.05$. Means (± SD) of all dependent variables are provided in Table S2.

Prior to analysis, all dependent variables to be included in the models were tested for possible correlations using Spearman's rank correlation (*cor.test* function) separated by life stage (i.e., larvae, juveniles). Variables with a correlation coefficient higher than 0.7 were considered strongly correlated and were thus, elimintaed to minimize redundancy (Fielding and Haworth, 1995; Chin, 1998) (Tables S3 and S4).

Parametric assumptions were tested using Kolmogorov-Smirnov tests (*lillie.test* function in the nortest package; Gross and Ligges, 2015) for normality as well as visual inspection of Q-Q plots made with *ggnorm* function, and Bartlett's tests (*bartlett.test* function in the car package; Fox et al., 2007) for homogeneity of variances. We fitted linear (LMM) and generalized mixed models (GLMM) including both fixed and random effects. In all models, likelihood ratio tests were used to determine the significance of each factor. We ran *lmer* and *glmer* functions in the lme4 package (Bates et al., 2019) for parametric and non-parametric data, respectively. Normally and non-normally distributed data were modelled with a Gaussian and Gammy distribution, respectively. Larval body mass and CORT values were log-transformed to fit parametric assumptions. First, we generated a global model for each dependent variable observed including rearing "temperature", "treatment" (MP, Cellulose, and Control) and their interaction as fixed factors. We included the variable 'aquarium' as a random factor in order to address dependencies in the data. Then, we conducted stepwise model selection by generating submodels from the global model according to the procedure of Zuur et al. (2009). The Akaike information criterion was used to assess the goodness of fit of each model. Finally, we determined Δ-values (AIC-differences) compared to the global models and the null models (i.e., only including the intercept). Estimates and p-values of each variable were provided by the best-fitting model (Table 1).

Differences in MP accumulation among treatments were analyzed visually and descriptively due to the low number of samples taken from one replicate (i.e., larvae: N = 1; juveniles_total: N = 2; juveniles_dissection: N = 2). We here provide mean (± SD), minimum, and maximum values of counted MP particles per treatment as well as the mean (± SD) number of MP particles $\times g^{-1}$ per treatment (Table S5). We provide both a figure showing size-corrected particle counts treatment (Fig. 3) and a figure showing the absolute MP counts per treatment (Fig. S2).

3. Results

A raw data table in xlsx format, including all original measurements, will be deposited in Figshare under DOI:XXX after acceptance.

3.1.1 Effects of MP treatment and rearing temperature on larval X. laevis

Length of larval period varied among all groups and, thus, was influenced by both treatment and rearing temperature (Table 1). Larval period was shortened at high temperature and was longest in the Cellulose treatment at 25 °C (Table S2). Differences among fiber treatments were more pronounced at 28 °C.

Snout-vent length and growth rate were significantly influenced by the fiber treatment and rearing temperature (Fig. 1AB; Table 1), but not by the interactive effect of both. Whereas SVL was on average 9.55 % shorter in larvae from the MP treatment compared to the control group, body mass did not differ between the treatments (Fig. 1AC; Table 1). Higher temperature caused on average a 14.71% reduction in growth rate and a 7.56% reduction in SVL (Table 1). Larvae from the MP treatment revealed an average increment in growth rate of 17.36 % compared to the control group. Body mass decreased on average by 24.42 % with rearing temperature across treatments. The reduction was most pronounced in the MP treatment (-25.99 %).

Body condition (i.e., SMI) and CORT levels were significantly higher in larvae exposed to MP and Cellulose (Fig. 1DE; Table 1). In contrast, temperature had no effect on body condition and CORT levels. Larvae from the MP treatment revealed a 41.17 % higher SMR in comparison to the control group (Fig. 1F; Table 1). SMR increased with temperature in all treatments (Fig. 1F) and was lowest in the Cellulose treatment at 25 °C, whereas it was highest in the MP treatment at 28 °C (Fig. 1F; Table S2).

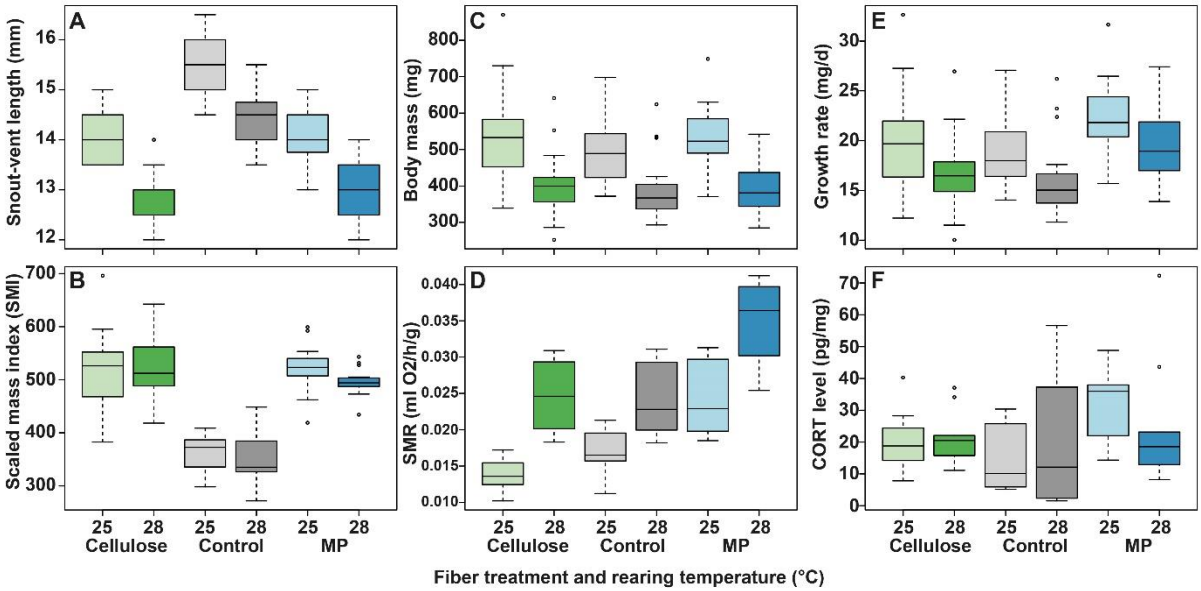

Fig. 1. Effects of MP ingestion during development on **A** snout-vent length (mm), **B** growth rate (mg × d^{-1})**, C** body mass (mg), **D** body condition (scaled mass index, SMI), **E** corticosterone level (pg × mg^{-1}), and **F** standard metabolic rate (SMR, mL O_2 × h^{-1} × g^{-1}), in *Xenopus laevis* larvae at developmental stage NF57. Box = 1. And 3. Quartiles. Whiskers = 1.5-fold interquartile range. Dots = outliers, minimum, and maximum values. Error bar = median.

Table 1. Estimates and standard errors (SE) of variables for best models derived from stepwise model selection procedures. We fitted linear and generalized mixed models. The global model included rearing temperature (°C), treatment (i.e., Control, MP, and Cellulose) and the interactive effect of temperature and treatment. Dependent variables were assessed in late larvae (i.e., developmental stage NF57) and juveniles (i.e., ten days after completing metamorphosis at NF66) of *Xenopus laevis*.

Life stage	Trait	Estimate	SE	P-value	N(n)	Δ AIC to global model	Δ to AIC null model
Larvae	**Larval period**				90(18)		
	(Intercept)	42.28	1.57	<**0.001**			
	MP	14.04	2.22	<**0.001**			
	Cellulose	8.15	2.22	<**0.001**			
	Temperature	-0.68	0.05	<**0.001**			
	MP*Temperature	-0.64	0.08	<**0.001**			
	Cellulose*Temperature	-0.28	0.08	**0.001**			
	best model **~ global model**					NA	268.96
	SVL				90(18)		
	(Intercept)	24.7	1.19	<**0.001**			
	MP	-1.43	0.16	<**0.001**			
	Cellulose	-1.46	0.16	<**0.001**			
	Temperature	-0.36	14.00	<**0.001**			
	best model						

	~ Treatment +Temperature					3.46	93.02
	log_Body mass				90(18)		
	(Intercept)	3.72	0.21	<**0.001**			
	Temperature	-0.04	0.01	<**0.001**			
	best model **~Temperature**					7.49	31.88
	GR				90(18)		
	(Intercept)	44.61	9.79	<**0.001**			
	MP	3.11	1.35	**0.037**			
	Cellulose	0.43	135	0.754			
	Temperature	-1.01	0.36	**0.015**			
	best model **~ Treatment + Temperature**					3.90	11.61
	SMI				90(18)		
	(Intercept)	356.03	12.93	<**0.001**			
	MP	152.76	18.28	<**0.001**			
	Cellulose	162.91	18.28	<**0.001**			
	best model **~ Treatment**					4.49	98.89
	SMR				90(18)		
	(Intercept)	-0.06	0.01	<**0.001**			
	MP	0.01	0.00	<**0.001**			
	Cellulose	-0.00	0.00	0.218			
	Temperature	0.00	0.00	<**0.001**			
	best model **~ Treatment + Temperature**					0.54	100.99
	log_CORT level				54(18)		
	(Intercept)	1.01	0.07	<**0.001**			
	MP	0.36	0.11	**0.001**			
	Cellulose	0.27	0.11	**0.015**			
	best model **~ Treatment**					16.23	4.49
Juveniles	**Body mass**				72(18)		
	(Intercept)	3606.47	447.91	<**0.001**			
	MP	-395.05	633.44	0.535			
	Cellulose	-2116.36	633.44	**0.001**			
	Temperature	-106.47	16.88	<**0.001**			
	MP*Temperature	19.19	23.87	0.424			
	Cellulose*Temperature	76.94	23.87	**0.001**			
	best model **~ global model**					NA	53.71
	SVL				72(18)		
	(Intercept)	40.50	3.99	<**0.001**			
	MP	-8.19	5.64	0.172			
	Cellulose	-11.53	5.64	0.063			
	Temperature	-0.83	0.15	<**0.001**			
	MP*Temperature	0.36	0.21	0.115			
	Cellulose*Temperature	0.4	0.21	0.058			
	best model **~ global model**					NA	47.21
	Relative body width				72(18)		
	(Intercept)	0.902	0.07	<**0.001**			
	MP	0.031	0.01	**0.012**			
	Cellulose	0.01	0.01	0.324			
	Temperature	-0.01	0.00	**0.008**			
	best model					2.92	16.01

	~ Treatment + Temperature						
	HSI				36(18)		
	(Intercept)	2.87	2.27	0.223			
	Temperature	-0.03	0.08	0.713			
	best model **~ Temperature**					1.84	2.86
	Relative forelimb length				72(18)		
	(Intercept)	-0.07	0.12	0.524			
	MP	0.49	0.16	**0.004**			
	Cellulose	0.01	0.16	0.940			
	Temperature	0.00	0.00	0.509			
	MP*Temperature	-0.018	0.01	**0.003**			
	Cellulose*Temperature	-0.000	0.01	0.937			
	best model **~ global model**					NA	2.30
	Relative hindlimb length				72(18)		
	(Intercept)	-0.12	0.07	0.093			
	MP	0.58	0.11	<**0.001**			
	Cellulose	0.09	0.11	0.389			
	Temperature	0.00	0.00	0.085			
	MP*Temperature	-0.02	0.00	<**0.001**			
	Cellulose*Temperature	-0.00	0.00	0.401			
	best model **~ global model**					NA	27.30
	Tibiofibula-to-femur ratio				72(18)		
	(Intercept)	1.38	0.11	<**0.001**			
	MP	0.02	0.01	0.213			
	Cellulose	0.01	0.01	0.432			
	Temperature	-0.01	0.00	**0.031**			
	best model **~ Treatment + Temperature**					3.61	1.46

3.1.2 Carry-over effects of larval MP exposure and rearing temperature in juvenile X. laevis

Larval rearing temperature had a carry-over effect on juvenile body mass and SVL, regardless of consumption of fibers. A higher rearing temperature caused on average an 8.54 % reduction in SVL and 27.55 % reduction in body mass (Table 1; Table S2). In contrast, there was no carry-over effect of the fiber treatments during larval development on SVL (Table 1; Table S2). Neither rearing temperature nor treatment during larval period affected the HSI (i.e., estimate for size of juvenile energy storages) (Table 1; Table S2).

Larval MP consumption and rearing temperature had a carry-over effect on juvenile body proportions. Bodies of juveniles from the MP treatment were on average 7.54 % wider compared to the control group (Table 1; Fig. 2D). Higher rearing temperature caused on average a 5.08% reduction in juvenile relative body width (Table 1; Fig. 2D). Relative forelimb and hindlimb length were significantly longer in juveniles that were exposed to MP during larval development (Table 1; Fig. 2AC). This effect, however, was overlaid by a significant interaction of treatment and rearing temperature which resulted in shorter relative limb lengths in specimens reared at 28 °C as larvae (Table 1; Fig. 2AC). The tibiofibula-to-femur (TFF) ratio as on average 2.57 % lower in juveniles that were reared at 28 °C during development (Fig. 2B; Table 1); this effect was independent of the treatment (Table 1).

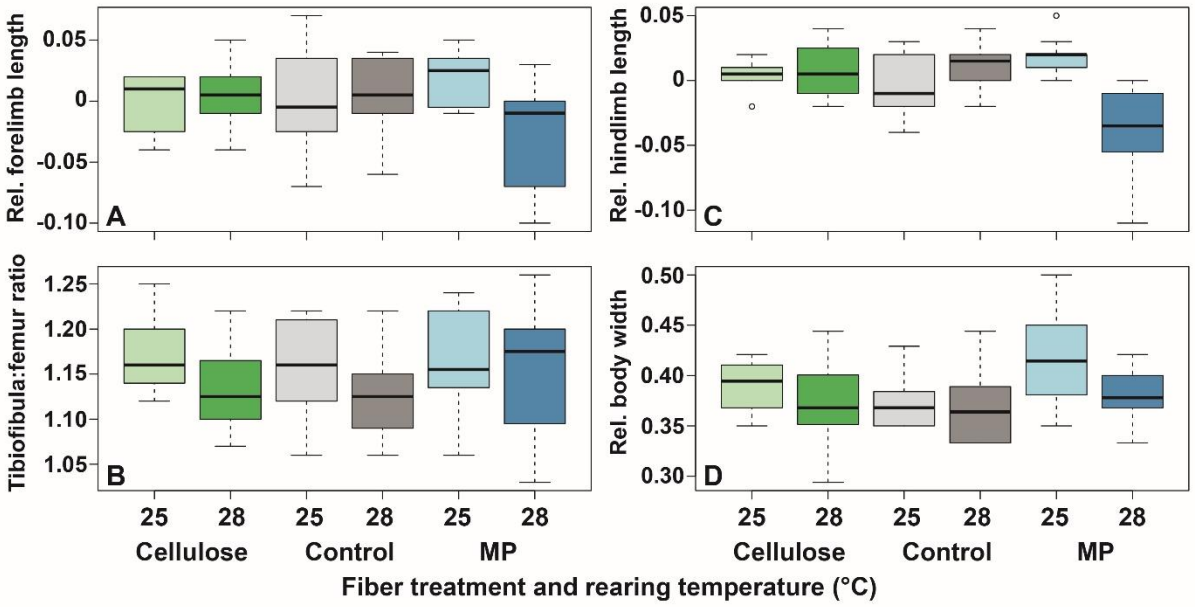

Fig. 2. Effects of MP ingestion during development on **A** relative forelimb length, **B** tibiofibula:femur ratio, **C** relative hindlimb length, and **D** relative body width in juveniles (i.e., ten days after completing metamorphosis at NF66) of *Xenopus laevis*. Box = 1. and 3. quartiles. Whiskers = 1.5-fold interquartile range. Dots = outliers, minimum, and maximum values. Error bar = median.

3.1.3 MP accumulation before and after metamorphosis

Before the start of the experiment, both food types as well as the Cellulose powder were checked for polyethylene MP particles used in the present study to control for contamination. Although some particles looked similar to the MP particles used in the present study, no polyethylene MP particles were found in food samples of the larval food nor in the juvenile food, or in the Cellulose powder (Fig. S1). Particles similar to polyethylene MP were smaller, flatter, or had a different surface than the polyethylene MP particles used in the present study (Fig. 3E).

Microplastics particles were found in both life stages of *X. laevis* (Fig. 3; Table S5), the amount, however, varied with treatment and temperature. In larvae at stage NF57, MP particles were found in high density in the MP treatment but not in the Control group (Fig. 3A; Table S5). The number of MP particles was higher in larvae reared at 28 °C compared to the larvae reared at 25 °C (25 °C: 177.83 particles × g^{-1}; 28 °C: 284.97 particles × g^{-1}). Larvae of the Cellulose treatment contained very few MP particles (25 °C: 9.92 particles × g^{-1}; 28 °C: 7.94 particles × g^{-1}). However, absolute MP particles found in the Cellulose treatment were extremely low and might be related to a similarity of the particles found in the food and so, rather to background noise than to contamination (Fig. S1).

In juveniles, MP particles were present in all sample types (i.e., whole bodies, gut, body remains). When whole bodies were analyzed, juveniles that were exposed to MP during larval development revealed accumulated MP particles. The mean number of accumulated particles was higher in juveniles that developed at 25 °C compared to those reared at 28 °C (25 °C: 16.53 particles × g^{-1}; 28 °C: 6.42 particles × g^{-1}). In whole bodies, we found neglectable amounts of MP particles in the Control (25 °C: 0.65 particles × g^{-1}; 28 °C: 0.86 particles × g^{-1}) and Cellulose treatment (25 °C: 0.65 particles × g^{-1}; 28 °C: none; Table S4; Fig. 3B). Independent of temperature and treatment, more MP particles were detected in the gut than in the body remains. Guts of juveniles exposed to MP during larval development contained the highest number of accumulated MP particles. The mean number of accumulated particles in gut samples was

higher in juveniles that developed at 25 °C (25 °C: 888.7 particles × g^{-1}; 28 °C: 521.29 particles × g^{-1}). The guts of juveniles of the other treatments contained considerably less or no MP particles (Control 25 °C: 35.14 particles × g^{-1}; Control 28 °C: 47.61 particles × g^{-1}; Cellulose 25 °C: 22.42 particles × g^{-1}; Cellulose 28 °C: none). Absolute MP particle counts in the body remains were neglectable across treatments and temperatures and can be related to background noise (Table S5; Fig 3D; Fig. S1).

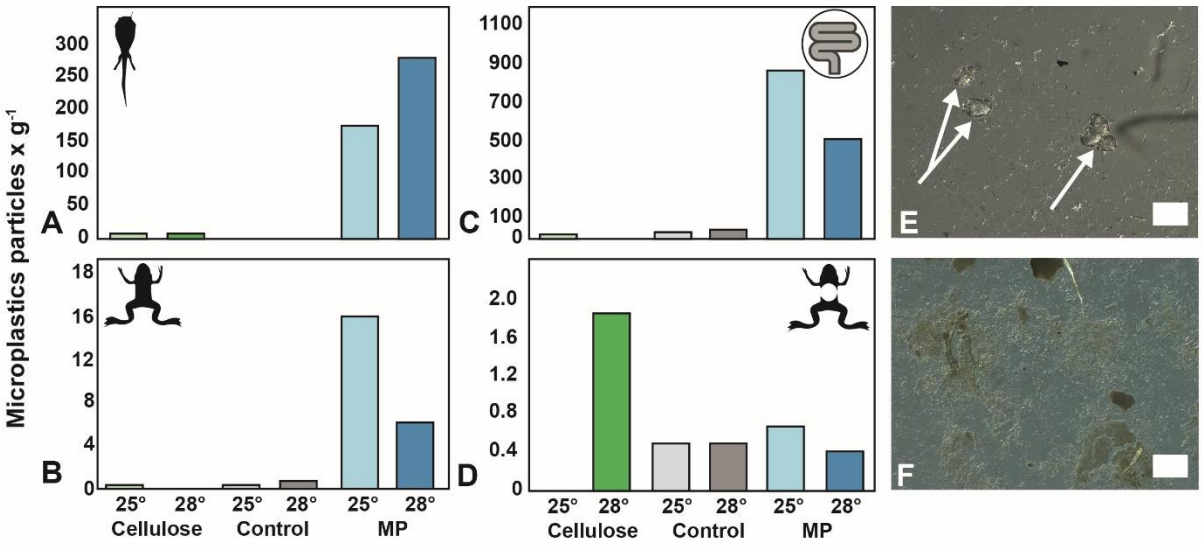

Fig. 3. Mean number of MP particles × g^{-1} per treatment in late larvae (i.e., developmental stage NF57,) and in juveniles (i.e., ten days after completing metamorphosis at NF66) in *Xenopus laevis*. One larva and four juveniles of each aquarium were randomly selected and analyzed, respectively. The **A** larvae (N = 18) and half of the **B** juveniles (N = 36) were processed and analyzed in total, whereas in the second half of the juveniles (N = 36) the guts were dissected. Both **C** the guts and **D** the body remnants after gut dissection were analyzed individually. Light microscopic pictures of **E** the MP treatment and **F** the control group at 400x magnification (Axio Imager.M2, Zeiss, Germany). Width of white rectangle: 100 µm. White arrows: MP particles.

4. Discussion

4.1 Sublethal effects of MP and rearing temperature on larval X. laevis

Despite the ubiquitous presence of MP in freshwater habitats typically encountered by amphibians (Talbot and Chang, 2022; Buss et al., 2022), toxicological effects of MP pollution are largely unknown for amphibians (rev. in Prokić et al., 2021; rev. in Burgos-Aceves et al., 2022). Here, we show that ingestion of polyethylene MP led to sublethal effects on growth, development, and metabolism in larval *X. laevis*. Larvae exposed to MP had a shorter larval period, indicating that MP ingestion led to an acceleration in developmental rate. In amphibian larvae, developmental acceleration in response to environmental stimuli is achieved via the activation of the neuroendocrine stress axis resulting in an increase in glucocorticoid hormone (i.e., CORT) production (Gomez-Mestre et al., 2013; Kulkarni et al., 2017). As CORT acts synergistically with the thyroid hormone to trigger amphibian metamorphosis (Kulkarni and Buchholz, 2012; Sterner and Buchholz, 2022), developmental rate increases with increasing CORT levels, ultimately resulting in a shorter larval period. Indeed, in larvae exposed to MP, we found higher endogenous CORT levels, suggesting that the faster developmental rate observed therein was mediated by increased production of the stress hormone. Besides developmental rate, CORT regulates metabolic processes such as energy mobilization and allocation as well as nutrient homeostasis (Kirschman et al., 2017). Thus, increased CORT levels are concomitant with higher metabolic activity (Wack et al., 2012; Kulkarni et al., 2017).

In the present study, larvae exposed to MP revealed an increased metabolic rate suggesting that elevated CORT levels caused associated increases in metabolic activity. Even if all effects found can be considered as sublethal, both increased metabolic activity and glucocorticoid hormone production are closely linked to (chronic) inflammation and oxidative stress (Burraco et al., 2013) that, in turn, might cause various deleterious effects on individual, cellular, and molecular level which eventually led to decreased overall health (Franzellitti et al., 2019). Studies on fish and aquatic invertebrates, particularly filter feeders, demonstrated that particularly MP accumulation in the gut caused oxidative stress (Zhao et al., 2021: *Danio rerio*; Liu et al., 2022: *Daphnia magna*) that led to histopathological damage of the digestive tract (Han et al., 2022: *Procambarus clarkia;* Chen et al., 2022: *Daphnia magna*) and resulted in inflammatory effects (Pei et al., 2022: *Danio rerio*). As the gut is the functional link between energy intake and energy allocation (Ruthsatz et al., 2022a, 2019), any disruption may result in adverse effects on food intake and/or nutrient absorption and thus, metabolic disorders with consequences for growth, development, immune functioning, and ultimately survival. Consequently, future studies should consider the gut as a suitable candidate to explore consequences of MP ingestion at multiple levels in amphibians.

So far, most studies on the effect of MP in amphibians have focused on evaluating the effect of MP alone (rev. in Burgos-Aceves et al., 2022) without considering the interaction with other environmental stressors, which would provide more complex and realistic exposure scenarios (rev. in Crain et al., 2008; Silva et al., 2022). The present study addressed the interactive effects of MP exposure and different rearing temperatures in order to test whether thermal stress might mediate/increase the toxicity of MP in amphibians. Indeed, there was a synergistic effect of MP and temperature on larval period. Larvae exposed to MP showed an even shorter larval period, when reared at 28 °C. In contrast, Silva et al. (2022) found an antagonistic effect of MP exposure and thermal stress on developmental rate in the harlequin fly (*Chironomus riparius*). In addition, two recent studies on the Cladoceran species *Daphnia magna* and *Daphnia pulex* could demonstrate a synergistic effect of temperature and MP exposure on survival rate (Jaikumar et al., 2018; Serra et al., 2020). However, despite the interactive effect of MP and rearing temperature on larval period, we did not observe a temperature mediated effect of MP on growth, survival, or the physiological parameters studied. Three hypotheses can explain these results: First, the selected higher temperature (i.e., 28 °C) may have not been stressful enough to induce interactive effects with MP exposure. Second, the interactive effect of MP and temperature might vary with MP concentration as demonstrated in microalgae for low and high MP exposures in combination with higher temperatures that led to an antagonistic and synergistic effect on the growth rate, respectively (Zhang et al., 2022). Third, some studies have shown that tadpoles can egest MP particles relatively fast (Hu et al., 2016; De Felice et al., 2018). As we found a higher number of MP particles in tadpoles reared at 28 °C indicating an increase in ingestion with temperature possibly due to higher energetic demands since metabolic rate scales positively with increasing ambient temperature in ectothermic animals such as amphibians (e.g., Burraco et al., 2018; Rowe and Crandall, 2018; but not: Burraco and Gomez-Mestre, 2016). We therefore suggest that gut passage time of food items and MP particles and so, egestion of both might also be faster at higher temperatures (Carreira et al., 2016). However, assessing gut passage time of MP particle in relation to temperature was outside the scope of the present study. Therefore, further research on the interplay between temperature, MP ingestion and egestion (i.e., gut passage time), and derived metabolic changes is needed in order to better understand the physiological consequences of MP pollution for amphibians in global climate change reality.

4.2 Carry-over effects of MP exposure during larval development on juvenile morphology

Conditions experienced during one life stage can have profound effects on performance later in life (Goater, 1994; Pechenik et al., 1998; O'Connor et al., 2014). In amphibians, such carry-over effects on post-metamorphic performance have been demonstrated for many environmental factors experienced during larval development (e.g., Buss et al., 2021; ; Ruthsatz et al., 2020b; Räsänen et al., 2002; Beck and Congdon, 2001). In the present study, MP ingestion during larval stage led not only to higher CORT levels, higher SMR, and concomitant faster development of tadpoles, but also to changes in body proportions in juveniles. Froglets that were exposed to MP during larval development had wider bodies and relatively longer extremities. In contrast, extremities were shorter in juveniles of the MP treatment if larvae were reared at 28 °C; this could be due to an energetic mismatch at higher rearing temperatures during development: metabolic rate increases with ambient temperature in ectotherms such as amphibians, and so might ingestion rate in order to cover these higher energetic demands. Likewise, digestion and egestion rate increase with temperature (Carreira et al., 2016). As a result, the digestive efficiency might be reduced when food is processed and egested faster. This could be detrimental when the ingested food contains a large number of indigestible fibers such as MP particles. Consequently, less energy might be available for extremity ontogeny during metamorphosis, ultimately resulting in reduced extremity length at 28 °C. Such allometric carry-over effects on juvenile body proportions might have adverse effects on locomotor performance, food intake efficiency, and ultimately on fitness. For example, many anurans, including *X. laevis* use the forelimbs for food grasping, as well as to bring food items into their mouth (Gray et al., 1997; Anzeraey et al., 2017). The forelimbs need a certain length in order be able to fulfill these functions. On the other hand, longer forelimbs should produce higher drag during swimming and, therefore, might be biomechanically disadvantageous with regard to swimming performance. With regard to jumping, relatively longer hindlimbs result in a higher jumping performance by expanding the acceleration phase during take-off and therefore maximizing the amount of kinetic energy that is transferred to the trunk (e.g., Gans and Parsons, 1966). Assuming that the same principle that applies for jumping also applies for swimming, relatively shorter hindlimbs in specimens reared at 28 °C in the MP treatment (i.e., less propulsive force during swimming) might result in a decreased swimming performance. The increased relative body width in specimen exposed to MP during larval development likely increase this negative effect (higher drag during swimming). Consequently, the observed data indicate that potentially negative carry-over effects of MP pollution on body proportions become more pronounced with increasing temperature (as it, e.g., occurs with global warming).

4.3 First evidence for ontogenetic transfer of MP in amphibians across metamorphosis

MP are known to accumulate extensively in the digestive tract after ingestion (Lei et al., 2018; Bacchetta et al., 2021; da Costa Araujo and Malafaia, 2020; but not: Hu et al., 2016). However, during amphibian metamorphosis, the intestinal tract is completely remodeled (Hourdry et al., 1996; Shi, 2000), suggesting that accumulated MP could exit the metamorphosing body along with feces and dead intestinal cells. The present study is the first demonstrating for amphibians that MP can be ontogenically transferred from the larval to the juvenile stage across metamorphosis. Polyethylene MP particles in individuals exposed as tadpoles persisted in juvenile *X. laevis* even ten days after exposure stopped. In juvenile frogs, the highest (absolute and relative) amount of MP particles was detected in gut samples indicating that the particles remained accumulated in the intestinal tract regardless of the morphological changes during metamorphosis. Ontogenetic transfer of MP has been previously demonstrated in invertebrates with complex life cycles (e.g., Al-Jaibachi et al., 2019, 2018; Setyorini et al., 2021; Simakova et al., 2022; Michler-Kozma et al., 2022). For example, Al-Jaibachi et al. (2018) demonstrated that polystyrene MP beads are transferred from feeding to non-feeding life stages during metamorphosis in the *Culex pipiens* mosquito complex. However, our results are based on a species that differs in larval feeding behavior from other amphibian species and remains aquatic

after metamorphosis. To enable generalizations across amphibian species, more comprehensive research is required to further explore potential ontogenetic transfer pathways in amphibians.

5. Conclusion

The present study reveals that ingestion of polyethylene MP leads to sublethal effects on growth and development, increased levels of stress hormone, and elevated metabolic rate in larval *X. laevis*, resulting in carry-over effects on juvenile morphology. We further present the first evidence of ontogenetic transfer of MP from the larval to the juvenile stage. Our results are of relevant ecological significance because an ontogenetic transfer from an aquatic life stage to the juvenile stage in amphibians might be a possible pathway for MP from freshwater to terrestrial ecosystems. However, the research on MP prevalence and abundance in freshwater systems including typical amphibian habitats such as ponds and puddles is still limited, in contrast to marine studies (Li et al., 2018). Only few studies to date have assessed MP pollution in amphibian habitats and demonstrated that MP can be accumulated by amphibians under field conditions (larvae: Hu et al., 2022, 2018; Kolenda et al., 2020; rev. in da Costa Araujo et al., 2021; adults: Karaoğlu and Gül, 2020; Bacchetta et al., 2021; Mackenzie and Vladimirova, 2021; Pastorino et al., 2022). Spectroscopic techniques such as Fourier transform infrared spectroscopy (FTIR) and Raman spectroscopy could be applied (Xu et al., 2019; Ta and Babel, 2022) to assess the prevalence and abundance of MP in amphibian habitats, to determine the origin of these MP, to evaluate possible ontogenetic transfer pathways, and to investigate the role of amphibians in trophic transfer of MP in order to allow for generalizations and the development of effective conservation strategies.

6. Acknowledgements

We thank Miguel Vences for supporting this project and for useful discussions on the methods while conceiving this study. We thank Rafael Rico and Francisco Miranda for their guidance in the laboratory of the Estación Biológica de Doñana in Seville, Spain. We are particularly thankful to Jutta Dammann from the Universitätsklinikum Hamburg Eppendorf for her great commitment in the husbandry and breeding of *Xenopus laevis.* We thank Guilherme Malafaia for prolific discussions while conceiving this study and for providing useful methodological information. We thank Gabriele Keunecke for the help in the laboratory in Braunschweig. We are grateful to four anonymous reviewers for insightful and helpful comments on the manuscript. The study was financed by intramural funds of the Technische Universität Braunschweig.

7. Author contributions

KR conceived, designed, and supervised the study. KR, MD, and FB conducted the experiments. MD performed the morphometric measurements. FB carried out the microdissections of intestinal structures. AS and RM conducted the light microscopic analyses. KR and KE performed the statistical analysis and led the writing of the manuscript. All authors participated in manuscript editing and final approval.

8. Conflict of Interest

The authors declare that the research was conducted in the absence of any commercial or financial relationships that could be construed as a potential conflict of interest.

9. Statement of Ethics

The authors have no ethical conflicts to disclose. All applicable international, national and/or institutional guidelines for the care and use of animals were followed. The experiments followed the ARRIVE guidelines and were conducted under permission from the

Niedersächsisches Landesamt für Verbraucherschutz und Lebensmittelsicherheit, Germany (Gz. 33.19-42502-04-21/3705).

10. Funding

This research did not receive any specific grant from funding agencies in the public, commercial, or not-for-profit sectors. The study was financed by intramural funds of the Technische Universität Braunschweig.

11. References

Akdogan, Z., Guven, B., 2019. Microplastics in the environment: A critical review of current understanding and identification of future research needs. Environ. Pollut., 254, 113011. https://doi.org/10.1016/j.envpol.2019.113011.

Al-Jaibachi, R., Cuthbert, R.N., Callaghan, A., 2018. Up and away: ontogenic transference as a pathway for aerial dispersal of microplastics. Biol. Lett., 14(9), 20180479. https://doi.org/10.1098/rsbl.2018.0479.

Al-Jaibachi, R., Cuthbert, R.N., Callaghan, A., 2019. Examining effects of ontogenic microplastic transference on *Culex* mosquito mortality and adult weight. Sci. Total Environ., 651, 871-876. https://doi.org/10.1016/j.scitotenv.2018.09.236.

Anbumani, S., Kakkar, P., 2018. Ecotoxicological effects of microplastics on biota: a review. Environ. Sci. Pollut. R., 25, 14373-14396. https://doi.org/10.1007/s11356-018-1999-x.

Anzeraey, A., Aumont, M., Decamps, T., Herrel, A., Pouydebat, E., 2017. The effect of food properties on grasping and manipulation in the aquatic frog *Xenopus laevis*. J. Exp. Biol., 220(23), 4486-4491. https://doi.org/10.1242/jeb.159442.

Archard, G.A., Goldsmith, A.R., 2010. Euthanasia methods, corticosterone and haematocrit levels in *Xenopus laevis*: evidence for differences in stress?. Anim. Welf. 19(1), 85-92. https://doi.org/10.1017/S0962728600001202.

Bacchetta, R., Winkler, A., Santo, N., Tremolada, P., 2021. The toxicity of polyester fibers in *Xenopus laevis*. Water, 13(23), 3446. https://doi.org/10.3390/w13233446.

Balestrieri, A., Winkler, A., Scribano, G., Gazzola, A., Lastrico, G., Grioni, A., Pellitteri-Rosa, D., Tremolada, P., 2022. Differential effects of microplastic exposure on anuran tadpoles: A still underrated threat to amphibian conservation?. Environ. Poll., 303, 119137. https://doi.org/10.1016/j.envpol.2022.119137.

Bates, D., Mächler, M., Bolker, B., Walker, S., 2019. Fitting linear mixed-effects models using lme4. J. Stat. Softw., 67(1), 1-48. https://doi.org/10.18637/jss.v067.i01.

Beck, C.W., Congdon, J.D., 2001. Effects of age and size at metamorphosis on performance and metabolic rates of Southern Toad, *Bufo terrestris*, metamorphs. Funct. Ecol., 14(1), 32-38. https://doi.org/10.1046/j.1365-2435.2000.00386.x.

Bhattacharya, A., Khare, S.K., 2022. Ecological and toxicological manifestations of microplastics: current scenario, research gaps, and possible alleviation measures. J. Environ. Sci. Heal C, 38(1), 1-20. https://doi.org/10.1080/10590501.2019.1699379.

Bolger, T., Connolly, P.L., 1989. The selection of suitable indices for the measurement and analysis of fish condition. J. Fish Biol., 34(2), 171-182. https://doi.org/10.1111/j.1095-8649.1989.tb03300.x.

703 Borrelle, S.B., Rochman, C.M., Liboiron, M., Bond, A.L., Lusher, A., Bradshaw, H., Provencher, J.F.,
704 2017. Why we need an international agreement on marine plastic pollution. P. Natl. Acad. Sci.
705 USA, 114(38), 9994-9997. https://doi.org/10.1073/pnas.1714450114.

706 Bosch, J., Thumsová, B., López-Rojo, N., Pérez, J., Alonso, A., Fisher, M.C., Boyero, L., 2021.
707 Microplastics increase susceptibility of amphibian larvae to the chytrid fungus *Batrachochytrium*
708 *dendrobatidis*. Sci. Rep., 11(1), 22438. https://doi.org/10.1038/s41598-021-01973-1.

709 Boyero, L., López-Rojo, N., Bosch, J., Alonso, A., Correa-Araneda, F., Pérez, J., 2020. Microplastics
710 impair amphibian survival, body condition and function. Chemosphere, 244, 125500.
711 https://doi.org/10.1016/j.chemosphere.2019.125500.

712 Buchholz, D.R., 2017. *Xenopus* metamorphosis as a model to study thyroid hormone receptor function
713 during vertebrate developmental transitions. Mol. Cell. Endocrinol., 459, 64-70.
714 https://doi.org/10.1016/j.mce.2017.03.020.

715 Burgos-Aceves, M.A., Faggio, C., Betancourt-Lozano, M., González-Mille, D.J., Ilizaliturri-Hernández,
716 C.A., 2022. Ecotoxicological perspectives of microplastic pollution in amphibians. J. Toxicol. Env,
717 Heal. B, 1-17. https://doi.org/10.1080/10937404.2022.2140372.

718 Burraco, P., Duarte, L.J., and Gomez-Mestre, I., 2013. Predator-induced physiological responses in
719 tadpoles challenged with herbicide pollution. Curr. Zool., 59(4), 475-484.
720 https://doi.org/10.1093/czoolo/59.4.475.

721 Burraco, P., Gomez-Mestre, I., 2016. Physiological stress responses in amphibian larvae to multiple
722 stressors reveal marked anthropogenic effects even below lethal levels. Physiol. Biochem. Zool., 89(6),
723 462-472. https://doi.org/10.1086/688737.

724 Burraco, P., Iglesias-Carrasco, M., Cabido, C., Gomez-Mestre, I., 2018. Eucalypt leaf litter impairs
725 growth and development of amphibian larvae, inhibits their antipredator responses and alters their
726 physiology. Conserv. Physiol., 6(1), coy066. https://doi.org/10.1093/conphys/coy066.

727 Buss, N., Swierk, L., Hua, J., 2021. Amphibian breeding phenology influences offspring size and
728 response to a common wetland contaminant. Front. Zool., 18(1), 31. https://doi.org/10.1186/s12983-
729 021-00413-0 .

730 Buss, N., Sander, B., Hua, J., 2022. Effects of polyester microplastic fiber contamination on amphibian–
731 trematode interactions. Environ. Toxicol.Chem., 41(4), 869-879. https://doi.org/10.1002/etc.5035.

732 Carreira, B.M., Segurado, P., Orizaola, G., Gonçalves, N., Pinto, V., Laurila, A., Rebelo, R., 2016.
733 Warm vegetarians? Heat waves and diet shifts in tadpoles. Ecology, 97(11), 2964-2974.
734 https://doi.org/10.1002/ecy.1541.

735 Castro-Castellon, A.T., Horton, A.A., Hughes, J.M.R., Rampley, C., Jeffers, E.S., Bussi, G., Whitehead,
736 P., 2021. Ecotoxicity of microplastics to freshwater biota: Considering exposure and hazard across
737 trophic levels. Sci. Total Environ., 816, 151638. https://doi.org/10.1016/j.scitotenv.2021.151638.

738 Chen, C.C., Shi, Y., Zhu, Y., Zeng, J., Qian, W., Zhou, S., Ma, J., Pan, K., Jiang, Y., Tao, Y., Zhu, X.,
739 2022. Combined toxicity of polystyrene microplastics and ammonium perfluorooctanoate to *Daphnia*
740 *magna*: Mediation of intestinal blockage. Water Res., 219, 118536.
741 https://doi.org/10.1016/j.watres.2022.118536.

742 Chin, W.W., 1998. The partial least squares approach to structural equation modeling. In: Marcoulides,
743 G.A. (Ed), Modern methods for business research. Lawrence Erlbaum Associates Publishers, London,
744 pp. 295-336.

Crain, C.M., Kroeker, K., Halpern, B.S., 2008. Interactive and cumulative effects of multiple human stressors in marine systems. Ecol. Lett., 11(12), 1304-1315. https://doi.org/10.1111/j.1461-0248.2008.01253.x.

Curtis, A.N., Bidart, M.G., 2021. Increased temperature influenced growth and development of *Lithobates pipiens* tadpoles exposed to leachates of the invasive plant european buckthorn (*Rhamnus cathartica*) and a triclopyr herbicide. Environ. Toxicol. Chem., 40(9), 2547-2558. https://doi.org/10.1002/etc.5142.

da Costa Araújo, A.P., Malafaia, G., 2020. Can short exposure to polyethylene microplastics change tadpoles' behavior? A study conducted with neotropical tadpole species belonging to order anura (*Physalaemus cuvieri*). J. Hazard. Mater.s, 391, 122214. https://doi.org/10.1016/j.jhazmat.2020.122214.

da Costa Araújo, A.P., de Melo, N.F.S., de Oliveira Junior, A.G., Rodrigues, F.P., Fernandes, T., de Andrade Vieira, J.E., Rocha, T.L., Malafaia, G., 2020a. How much are microplastics harmful to the health of amphibians? A study with pristine polyethylene microplastics and *Physalaemus cuvieri*. J. Hzard. Mater., 382, 121066. https://doi.org/10.1016/j.jhazmat.2019.121066.

Da Costa Araújo, A.P., Gomes, A.R., Malafaia, G., 2020b. Hepatotoxicity of pristine polyethylene microplastics in neotropical *Physalaemus cuvieri* tadpoles (Fitzinger, 1826). J. Hazard. Mater., 386, 121992. https://doi.org/10.1016/j.jhazmat.2019.121992.

Da Costa Araújo, A.P., Rocha, T.L., e Silva, D.D.M., Malafaia, G., 2021. Micro (nano) plastics as an emerging risk factor to the health of amphibian: A scientometric and systematic review. Chemosphere, 283, 131090. https://doi.org/10.1016/j.chemosphere.2021.131090.

da Costa Araújo, A. P., da Luz, T. M., Ahmed, M. A. I., Ali, M. M., Rahman, M. M., Nataraj, B., ... & Malafaia, G. (2023). Toxicity assessment of polyethylene microplastics in combination with a mix of emerging pollutants on *Physalaemus cuvieri* tadpoles. J. Environ. Sci., 127, 465-482.

Da Silva, A.P.A., de Oliveira, C.D.L., Quirino, A.M.S., da Silva, F.D.M., de Aquino Saraiva, R., Silva-Cavalcanti, J.S., 2018. Endocrine disruptors in aquatic environment: effects and consequences on the biodiversity of fish and amphibian species. Aquat.- Sci. Technol., 6(1), 35-51. https://doi.org/10.5296/ast.v6i1.12565.

De Felice, B., Bacchetta, R., Santo, N., Tremolada, P.,Parolini, M., 2018. Polystyrene microplastics did not affect body growth and swimming activity in *Xenopus laevis* tadpoles. Environ. Sci, Pollut. R., 25(34), 34644-34651. https://doi.org/10.1007/s11356-018-3408-x.

Diepens, N.J., Koelmans, A.A., 2018. Accumulation of plastic debris and associated contaminants in aquatic food webs. Environ. Sci. Technol., 52(15), 8510-8520. https://doi.org/10.1021/acs.est.8b02515.

Fielding, A.H., Haworth, P.F., 1995. Testing the generality of bird-habitat models. Conserv. Biol., 9(6), 1466-1481. https://doi.org/10.1046/j.1523-1739.1995.09061466.x.

Fox, J., Bates, D., Firth, D., Friendly, M.,Gorjanc, G., Graves, S., Heiberger, R., Monette, G., Nilsson, H., Ripley, B., Weisberg, S., Zeleis, A., 2007. The car package. R Foundation for Statistical Computing, 1109, 1431.

Franzellitti, S., Canesi, L., Auguste, M., Wathsala, R.H.G.R., Fabbri, E., 2019. Microplastic exposure and effects in aquatic organisms: a physiological perspective. Environ. Toxicol. Phar., 68, 37-51. https://doi.org/10.1016/j.etap.2019.03.009.

Gans, C., Parsons, T.S., 1966. On the origin of the jumping mechanism in frogs. Evolution, 20(1), 92-99. https://doi.org/10.2307/2406151.

Goater, C.P., 1994. Growth and survival of postmetamorphic toads: interactions among larval history, density, and parasitism. Ecology, 75(8), 2264-2274. https://doi.org/10.2307/1940882.

790 Gomez-Mestre, I., Pyron, R.A., Wiens, J.J., 2012. Phylogenetic analyses reveal unexpected patterns in
791 the evolution of reproductive modes in frogs. Evol. Internat. J. Org. Evol., 66(12), 3687-3700.
792 https://doi.org/10.1111/j.1558-5646.2012.01715.x.

793 Gomez-Mestre, I., Kulkarni, S., Buchholz, D.R., 2013. Mechanisms and consequences of developmental
794 acceleration in tadpoles responding to pond drying. PloS one, 8(12), e84266.
795 https://doi.org/10.1371/journal.pone.0084266.

796 Gray, L.A., O'Reilly, J.C., Nishikawa, K.C., 1997. Evolution of forelimb movement patterns for prey
797 manipulation in anurans. J. Exp. Zool., 277(6), 417-424. DOI: 10.1002/(sici)1097-
798 010x(19970415)277:6<417::aid-jez1>3.0.co;2-r

799 Gross, J., Ligges, U., 2015. Package 'nortest'. Five omnibus tests for testing the composite hypothesis
800 of normality.

801 Hale, R.C., Seeley, M.E., La Guardia, M.J., Mai, L., Zeng, E.Y., 2020. A global perspective on
802 microplastics. J. Geophys. Res.-Oceans, 125(1), e2018JC014719.
803 https://doi.org/10.1029/2018JC014719.

804 Han, M., Gao, T., Liu, G., Zhu, C., Zhang, T., Sun, M., Li, J., Si, Q., Jiang, Q., 2022. The effect of a
805 polystyrene nanoplastic on the intestinal microbes and oxidative stress defense of the freshwater
806 crayfish, *Procambarus clarkii*. Sci. Total Environ., 833, 155722.
807 https://doi.org/10.1016/j.scitotenv.2022.155722.

808 Hartmann, N.B., Rist, S., Bodin, J., Jensen, L.H.S., Schmidt, S.N., Mayer, P., Meibom, A., Baun, A.,
809 2017. Microplastics as vectors for environmental contaminants: Exploring sorption, desorption, and
810 transfer to biota. Integr. Environ. Asses., 13(3), 488-493. https://doi.org/10.1002/ieam.1904.

811 Hartmann, N.B., Hüffer, T., Thompson, R.C., Hassellöv, M., Verschoor, A., Daugaard, A.E., Rist, S.,
812 Karlsson, T., Brennholt, N., Cole, M., Herrling, M.P., Hess, M.C., Ivleva, N.P., Lusher, M.L., Wagner,
813 M., 2019. Are we speaking the same language? Recommendations for a definition and categorization
814 framework for plastic debris. Environ. Sci. Technol. 53 (3), 1039-1047.
815 https://doi.org/10.1021/acs.est.8b05297.

816 Hastings, D., Burggren, W., 1995. Developmental changes in oxygen consumption regulation in larvae
817 of the South African clawed frog *Xenopus laevis*. J. E.xp. Biol., 198(12), 2465-2475.
818 https://doi.org/10.1242/jeb.198.12.2465.

819 Hernández, S.E., Sernia, C., Bradley, A.J., 2012. The effect of three anaesthetic protocols on the stress
820 response in cane toads (*Rhinella marina*). Vet. Anaesth. Analg., 39(6), 584-590.
821 https://doi.org/10.1111/j.1467-2995.2012.00753.x.

822 Hocking, D.J., Babbitt, K.J., 2014. Amphibian contributions to ecosystem services. Herpetol. Conserv.
823 Bio., 9(1), 1-17.

824 Horton, A.A., Walton, A., Spurgeon, D.J., Lahive, E., Svendsen, C., 2017. Microplastics in freshwater
825 and terrestrial environments: evaluating the current understanding to identify the knowledge gaps and
826 future research priorities. Sci. Total Environ., 586, 127-141.
827 https://doi.org/10.1016/j.scitotenv.2017.01.190.

828 Hourdry, J., L'Hermite, A., Ferrand, R., 1996. Changes in the digestive tract and feeding behavior of
829 anuran amphibians during metamorphosis. Physiol. Zool., 69(2), 219-251.
830 https://doi.org/10.1086/physzool.69.2.30164181.

831 Htun-Han, M., 1978. The reproductive biology of the dab *Limanda limanda* (L.) in the North Sea:
832 gonosomatic index, hepatosomatic index and condition factor. J. Fish Biol., 13(3), 369-378.
833 https://doi.org/10.1111/j.1095-8649.1978.tb03445.x.

834 Hu, L., Su, L., Xue, Y., Mu, J., Zhu, J., Xu, J., Shi, H., 2016. Uptake, accumulation and elimination of
835 polystyrene microspheres in tadpoles of *Xenopus tropicalis*. Chemosphere, 164, 611-617.
836 https://doi.org/10.1016/j.chemosphere.2016.09.002.

837 Hu, L., Chernick, M., Hinton, D.E., Shi, H., 2018. Microplastics in small waterbodies and tadpoles from
838 Yangtze River Delta, China. Envir. Sci. Technol., 52(15), 8885-8893.
839 https://doi.org/10.1021/acs.est.8b02279.

840 Hu, L., Fu, J., Zheng, P., Dai, M., Zeng, G., Pan, X., 2022. Accumulation of microplastics in tadpoles
841 from different functional zones in Hangzhou Great Bay Area, China: Relation to growth stage and
842 feeding habits. J, Hazard. Mater., 424, Part D, 127665. https://doi.org/10.1016/j.jhazmat.2021.127665.

843 IUCN, 2022. The IUCN Red List of Threatened Species. Version 2022-1. https://www.iucnredlist.org
844 (downloaded on 31 July 2022).

845 Jaikumar, G., Baas, J., Brun, N. R., Vijver, M. G., & Bosker, T. (2018). Acute sensitivity of three
846 Cladoceran species to different types of microplastics in combination with thermal stress. *Environ.*
847 *Poll.*, *239*, 733-740. https://doi.org/10.1016/j.envpol.2018.04.069.

848 Jelodar, H.T., Fazli, H., 2012. Monthly changes in condition, hepatosomatic index and bioavailability
849 in frogs (*Rana ridibunda*). Res. J. Biol., 2(1), 29-34.

850 Karaoğlu, K., Gül, S., 2020. Characterization of microplastic pollution in tadpoles living in small water-
851 bodies from Rize, the northeast of Turkey. Chemosphere, 255, 126915.
852 https://doi.org/10.1016/j.chemosphere.2020.126915.

853 Kirschman, L J., McCue, M.D., Boyles, J.G., Warne, R.W., 2017. Exogenous stress hormones alter
854 energetic and nutrient costs of development and metamorphosis. J. Exp.Biol., 220(18), 3391-3397.
855 https://doi.org/10.1242/jeb.164830.

856 Kirstein, I.V., Kirmizi, S., Wichels, A., Garin-Fernandez, A., Erler, R., Löder, M., Gerdts, G., 2016.
857 Dangerous hitchhikers? Evidence for potentially pathogenic *Vibrio* spp. on microplastic particles. Mari.
858 Environ. Res., 120, 1-8. https://doi.org/10.1016/j.marenvres.2016.07.004.

859 Koelmans, A.A., Nor, N.H.M., Hermsen, E., Kooi, M., Mintenig, S.M., De France, J., 2019.
860 Microplastics in freshwaters and drinking water: Critical review and assessment of data quality. Water
861 Res., 155, 410-422. https://doi.org/10.1016/j.watres.2019.02.054.

862 Kolenda, K., Kuśmierek, N., Pstrowska, K., 2020. Microplastic ingestion by tadpoles of pond-breeding
863 amphibians – first results from Central Europe (SW Poland). Environ. Sci. Pollut. R., 27(26), 33380-
864 33384. https://doi.org/10.1007/s11356-020-09648-6.

865 Kratina, P., Watts, T.J., Green, D.S., Kordas, R.L., O'Gorman, E.J., 2019. Interactive effects of warming
866 and microplastics on metabolism but not feeding rates of a key freshwater detritivore. Environ.
867 Pollut., 255, Part 2, 113259. https://doi.org/10.1016/j.envpol.2019.113259.

868 Kulkarni, S.S., Buchholz, D.R., 2012. Beyond synergy: corticosterone and thyroid hormone have
869 numerous interaction effects on gene regulation in *Xenopus tropicalis* tadpoles. Endocrinology, 153(11),
870 5309-5324. DOI: 10.1210/en.2012-1432.

871 Kulkarni, S.S., Denver, R.J., Gomez-Mestre, I., Buchholz, D.R., 2017. Genetic accommodation via
872 modified endocrine signalling explains phenotypic divergence among spadefoot toad species. Nat.
873 Commun., 8(1), 1-7. https://doi.org/10.1038/s41467-017-00996-5.

874 Lei, L., Wu, S., Lu, S., Liu, M., Song, Y., Fu, Z., Shi, H., Raley-Susman, K.M., He, D., 2018.
875 Microplastic particles cause intestinal damage and other adverse effects in zebrafish *Danio rerio* and
876 nematode *Caenorhabditis elegans*. Sci.Total Environ., 619-620, 1-8.
877 https://doi.org/10.1016/j.scitotenv.2017.11.103.

878 Li, J., Liu, H., Chen, J.P., 2018. Microplastics in freshwater systems: A review on occurrence,
879 environmental effects, and methods for microplastics detection. Water Res., 137, 362-374.
880 https://doi.org/10.1016/j.watres.2017.12.056.

881 Liu, Y., Zhang, J., Zhao, H., Cai, J., Sultan, Y., Fang, H., Zhang, B., Ma, J., 2022. Effects of polyvinyl
882 chloride microplastics on reproduction, oxidative stress and reproduction and detoxification-related
883 genes in *Daphnia magna*. Comp. Biochem. Physiol. C, 254, 109269.
884 https://doi.org/10.1016/j.cbpc.2022.109269.

885 Mackenzie, C.M., Vladimirova, V., 2021. Preliminary study and first evidence of presence of
886 microplastics in terrestrial herpetofauna from Southwestern Paraguay. Studies on Neotropical Fauna and
887 Environment, 58(1), 16-24. https://doi.org/10.1080/01650521.2021.1895466.

888 Mausbach, J., Laurila, A., Räsänen, K., 2022. Context dependent variation in corticosterone and
889 phenotypic divergence of *Rana arvalis* populations along an acidification gradient. BMC Ecol.
890 Evol., 22(1), 11. https://doi.org/10.1186/s12862-022-01967-1.

891 Michler-Kozma, D.N., Kruckenfellner, L., Heitkamp, A., Ebke, K.P., Gabel, F., 2022. Uptake and
892 Transfer of Polyamide Microplastics in a Freshwater Mesocosm Study. Water, 14(6), 887.
893 https://doi.org/10.3390/w14060887.

894 Nieuwkoop, P.D., Faber, J., Gerhart, J., Kirschner, M., 1994. Normal table of *Xenopus laevis* (Daudin):
895 a systematical an chronological survey of the development from the fertilized egg till the end of
896 metamorphosis, firth ed. Garland Science. New York. https://doi.org/10.1201/9781003064565 .

897 Noyes, P.D., Lema, S.C.,2015. Forecasting the impacts of chemical pollution and climate change
898 interactions on the health of wildlife. Curr. Zool., 61(4), 669-689.
899 https://doi.org/10.1093/czoolo/61.4.669.

900 O'Connor, C.M., Norris, D.R., Crossin, G.T., Cooke, S.J. 2014. Biological carryover effects: linking
901 common concepts and mechanisms in ecology and evolution. Ecosphere, 5(3), 1-11.

902 Olesen, K.B., Stephansen, D.A., van Alst, N., Vollertsen, J., 2019. Microplastics in a stormwater pond.
903 Water, 11(7), 1466. https://doi.org/10.3390/w11071466.

904 Orlofske, S.A., Belden, L.K., Hopkins, W.A., 2017. Effects of *Echinostoma trivolvis* metacercariae
905 infection during development and metamorphosis of the wood frog (*Lithobates sylvaticus*). Com.
906 Biochem. Physiol. A, 203, 40-48. https://doi.org/10.1016/j.cbpa.2016.08.002.

907 Pastorino, P., Prearo, M., Di Blasio, A., Barcelò, D., Anselmi, S., Colussi, S., Alberti, S., Tedde, G.,
908 Dondo, A., Ottino, M., Pizzul, E., Renzi, M., 2022. Microplastics occurrence in the European common
909 frog (*Rana temporaria*) from Cottian Alps (Northwest Italy). Diversity, 14(2), 66.
910 https://doi.org/10.3390/d14020066.

911 Pechenik, J. A., Wendt, D. E., & Jarrett, J.N., 1998. Metamorphosis is not a new beginning: Larval
912 experience influences juvenile performance. Bioscience, 48(11), 901-910.
913 https://doi.org/10.2307/1313294.

914 Peck, M.A., Moyano, M. 2016. Measuring respiration rates in marine fish larvae: challenges and
915 advances. J. Fish Biol., 88(1), 173-205. https://doi.org/10.1111/jfb.12810.

916 Pei, X., Heng, X., Chu, W., 2022. Polystyrene nano/microplastics induce microbiota dysbiosis, oxidative
917 damage, and innate immune disruption in zebrafish. Microb. Pathog., 163, 105387.
918 https://doi.org/10.1016/j.micpath.2021.105387.

919 Peig, J., Green, A.J., 2009. New perspectives for estimating body condition from mass/length data: the
920 scaled mass index as an alternative method. Oikos, 118(12), 1883-1891. https://doi.org/10.1111/j.1600-
921 0706.2009.17643.x.

Peig, J., Green, A.J., 2010. The paradigm of body condition: a critical reappraisal of current methods based on mass and length. Funct. Ecol., 24(6), 1323-1332. https://doi.org/10.1111/j.1365-2435.2010.01751.x.

PlasticsEurope, 2022. Plastics – the Facts 2021: An analysis of European plastics production, demand and waste data. https://plasticseurope.org/knowledge-hub/plastics-the-facts-2021/ (accessed on 6 July 2022).

Prokić, M.D., Radovanović, T.B., Gavrić, J.P., Faggio, C., 2019. Ecotoxicological effects of microplastics: Examination of biomarkers, current state and future perspectives. TrAC--Trend. Anal. Chem., 111, 37-46. https://doi.org/10.1016/j.trac.2018.12.001.

Prokić, M.D., Gavrilović, B.R., Radovanović, T.B., Gavrić, J.P., Petrović, T.G., Despotović, S.G., Faggio, C., 2021. Studying microplastics: Lessons from evaluated literature on animal model organisms and experimental approaches. J. Hazard. Mater., 414, 125476. https://doi.org/10.1016/j.jhazmat.2021.125476.

Ramlochansingh, C., Branoner, F., Chagnaud, B.., Straka, H., 2014. Efficacy of tricaine methanesulfonate (MS-222) as an anesthetic agent for blocking sensory-motor responses in *Xenopus laevis* tadpoles. PloS one, 9(7), e101606. https://doi.org/10.1371/journal.pone.0101606.

Räsänen, K., Laurila, A., Merilä, J., 2002. Carry-over effects of embryonic acid conditions on development and growth of *Rana temporaria* tadpoles. Freshw. Biol., 47(1), 19-30. https://doi.org/10.1046/j.1365-2427.2002.00777.x.

Reichert, J., Tirpitz, V., Anand, R., Bach, K., Knopp, J., Schubert, P., Wilke, T., Ziegler, M,. 2021. Interactive effects of microplastic pollution and heat stress on reef-building corals. Environ. Pollut., 290, 118010. https://doi.org/10.1016/j.envpol.2021.118010.

Rehse, S., Kloas, W., Zarfl, C., 2016. Short-term exposure with high concentrations of pristine microplastic particles leads to immobilisation of *Daphnia magna*. Chemosphere, 153, 91-99. https://doi.org/10.1016/j.chemosphere.2016.02.133.

Rohr, J.R., Sesterhenn, T.M., Stieha, C., 2011. Will climate change reduce the effects of a pesticide on amphibians?: partitioning effects on exposure and susceptibility to contaminants. Glob. Chang. Biol., 17(2), 657-666. https://doi.org/10.1111/j.1365-2486.2010.02301.x.

Rowe, C.L., Crandall, E.A., 2018. The acute thermal respiratory response is unique among species in a guild of larval anuran amphibians – implications for energy economy in a warmer future. Sci Total Environ., 618, 229-235. https://doi.org/10.1016/j.scitotenv.2017.10.332.

Ruthsatz, K., Dausmann, K.H., Drees, C., Becker, L.I., Hartmann, L., Reese, J., Sabatino, N.M., Peck, M.A., Glos, J., 2018. Altered thyroid hormone levels affect body condition at metamorphosis in larvae of *Xenopus laevis*. J. Appl. Toxicol., 38(11), 1416-1425. https://doi.org/10.1002/jat.3663.

Ruthsatz, K., Giertz, L.M., Schröder, D., Glos, J., 2019. Chemical composition of food induces plasticity in digestive morphology in larvae of *Rana temporaria*. Biol. Open, 8(12), bio048041. https://doi.org/10.1242/bio.048041.

Ruthsatz, K., Dausmann, K.H., Drees, C., Becker, L.I., Hartmann, L., Reese, J., Reinhardt, S., Robinson, T., Sabatino, N.M., Peck, M.A., Glos, J., 2020a. Altered thyroid hormone levels affect the capacity for temperature-induced developmental plasticity in larvae of *Rana temporaria* and *Xenopus laevis*. J. Therm. Biol., 90, 102599. https://doi.org/10.1016/j.jtherbio.2020.102599.

Ruthsatz, K., Dausmann, K.H., Reinhardt, S., Robinson, T., Sabatino, N.M., Peck, M.A., Glos, J., 2020b. Post-metamorphic carry-over effects of altered thyroid hormone level and developmental temperature: physiological plasticity and body condition at two life stages in *Rana temporaria*. J. Comp. Physiol. B, 190(3), 297-315. https://doi.org/10.1007/s00360-020-01271-8 .

967 Ruthsatz, K., Domscheit, M., Engelkes, K., Vences, M., 2022a. Microplastics ingestion induces
968 plasticity in digestive morphology in larvae of *Xenopus laevis*. Com. Biochem. Physiol. A, 269, 111210.
969 https://doi.org/ 10.1016/j.cbpa.2022.111210.

970 Ruthsatz, K., Bartels, F., Stützer, D., Eterovick, P.C., 2022b. Timing of parental breeding shapes
971 sensitivity to nitrate pollution in the common frog *Rana temporaria*. J. Therm. Biol., 108, 103296.
972 https://doi.org/10.1016/j.jtherbio.2022.103296.

973 Ruthsatz, K., Eterovick, P.C., Bartels, F., Mausbach, J., 2023. Contributions of water-borne
974 corticosterone as one non-invasive biomarker in assessing nitrate pollution stress in tadpoles of *Rana*
975 *temporaria*. Gen. Comp. Endorc., 331, 114164. https://doi.org/10.1016/j.ygcen.2022.114164.

976 Schrank, I., Löder, M.G.J., Imhof, H.K., Moses, S.R., Heß, M., Schwaiger, J., Laforsch, C., 2022.
977 Riverine microplastic contamination in southwest Germany: A large-scale survey. Front. Earth Sci., 10.
978 https://doi.org/10.3389/feart.2022.794250.

979 Setyorini, L., Michler-Kozma, D., Sures, B., Gabel, F., 2021. Transfer and effects of PET microfibers
980 in *Chironomus riparius*. Sci. Total Environ., 757, 143735.
981 https://doi.org/10.1016/j.scitotenv.2020.143735.

982 Serra, T., Barcelona, A., Pous, N., Salvadó, V., Colomer, J., 2020. Synergistic effects of water
983 temperature, microplastics and ammonium as second and third order stressors on *Daphnia magna*.
984 Environ. Pollut., 267, 115439. https://doi.org/10.1016/j.envpol.2020.115439.

985 Shi, Y.B. (2000). Amphibian metamorphosis. Wiley-Liss, New York.

986 Silva, C.J.M., Machado, A.L., Campos, D., Soares, A.M.V.M., Pestana, J.L.T., 2022. Combined effects
987 of polyethylene microplastics and natural stressors on *Chironomus riparius* life-history traits. Environ.
988 Res., 213, 113641. https://doi.org/10.1016/j.envres.2022.113641.

989 Simakova, A., Varenitsina, A., Babkina, I., Andreeva, Y., Bagirov, R., Yartsev, V., Frank, Y., 2022.
990 Ontogenetic transfer of microplastics in bloodsucking mosquitoes *Aedes aegypti L*.(Diptera: Culicidae)
991 is a potential pathway for particle Distribution in the Environment. Water, 14(12), 1852.
992 https://doi.org/10.3390/w14121852.

993 Smith, B.D., Vail, K.J., Carroll, G.L., Taylor, M.C., Jeffery, N.D., Vemulapalli, T.H., Elliott, J.J., 2018.
994 Comparison of etomidate, benzocaine, and MS222 anesthesia with and without subsequent flunixin
995 meglumine analgesia in African clawed frogs (*Xenopus laevis*). J. Am. Assoc. Lab. Anim., 57(2), 202-
996 209.

997 Sterner, Z.R., Buchholz, D.R., 2022. Glucocorticoid receptor mediates corticosterone-thyroid hormone
998 synergy essential for metamorphosis in *Xenopus tropicalis* tadpoles. Gen. Comp. Endocr., 315, 113942.
999 https://doi.org/10.1016/j.ygcen.2021.113942.

1000 Stuart, S.N., Chanson, J.S., Cox, N.A., Young, B.E., Rodrigues, A.S.L., Fischman, D.L., Waller, R.W.,
1001 2004. Status and trends of amphibian declines and extinctions worldwide. Science, 306(5702), 1783-
1002 1786. https://doi.org/10.1126/science.1103538.

1003 Ta, A.T., Babel, S., 2022. Sources, Occurrence, and Analysis of Microplastics in Freshwater
1004 Environments: A Review, in: Ahamad, A., Singh, P., Tiwary, D. (Eds.), Plastic and Microplastic in the
1005 Environment: Management and Health Risks. Wiley Online Library, pp. 1-17.
1006 https://doi.org/10.1002/9781119800897.ch1.

1007 Talbot, R., Chang, H., 2022. Microplastics in freshwater: A global review of factors affecting spatial
1008 and temporal variations. Environ. Pollut., 292, 118393. https://doi.org/10.1016/j.envpol.2021.118393.

Thompson, R.C., Olsen, Y., Mitchell, R.P., Davis, A., Rowland, S.J., John, A.W.G., McGonigle, D., Russell, A.E., 2004. Lost at sea: where is all the plastic?. Science, 304(5672), 838-838. https://doi.org/10.1126/science.1094559

Venâncio, C., Melnic, I., Tamayo-Belda, M., Oliveira, M., Martins, M.A., Lopes, I., 2022. Polymethylmethacrylate nanoplastics can cause developmental malformations in early life stages of *Xenopus laevis*. Sci. Total Environ., 806, 150491. https://doi.org/10.1016/j.scitotenv.2021.150491.

Wack, C.L., DuRant, S.E., Hopkins, W.A., Lovern, M.B., Feldhoff, R.C., Woodley, S.K., 2012. Elevated plasma corticosterone increases metabolic rate in a terrestrial salamander. Comp. Biochem. Phys. A, 161(2), 153-158. https://doi.org/10.1016/j.cbpa.2011.10.017.

Wake, D.B., Vredenburg, V.T., 2008. Are we in the midst of the sixth mass extinction? A view from the world of amphibians. P. Natl. A. Sci.,105(supplement_1), 11466-11473. https://doi.org/10.1073/pnas.0801921105.

Wickham, H., 2009. Getting started with qplot. in: Wickham, H., ggplot2 . Springer, New York, pp. 9-26. https://doi.org/10.1007/978-0-387-98141-3_2.

Xu, J.L., Thomas, K.V., Luo, Z., Gowen, A.A., 2019. FTIR and Raman imaging for microplastics analysis: State of the art, challenges and prospects. TrAC Trend, Anal. Chem., 119, 115629. https://doi.org/10.1016/j.trac.2019.115629.

Zhao, Y., Qiao, R., Zhang, S., Wang, G., 2021. Metabolomic profiling reveals the intestinal toxicity of different length of microplastic fibers on zebrafish (*Danio rerio*). J. Hazard. Mater., 403, 123663. https://doi.org/10.1016/j.jhazmat.2020.123663.

Zhang, J., Kong, L., Zhao, Y., Lin, Q., Huang, S., Jin, Y., Ma, Z., Guan, W., 2022. Antagonistic and synergistic effects of warming and microplastics on microalgae: Case study of the red tide species *Prorocentrum donghaiense*. Environ. Pollut., 307, 119515. https://doi.org/10.1016/j.envpol.2022.119515.

Zuur, A.F., Ieno, E.N., Walker, N.., Saveliev, A.A., Smith, G.M., 2009. Mixed effects models and extensions in ecology with R (Vol. 574). New York.

Supplementary Material

Life in plastic, it's not fantastic: Sublethal effects of polyethylene microplastics ingestion throughout amphibian metamorphosis

Running title: Sublethal effects of microplastics on amphibians

Katharina Ruthsatz[1], Anja Schwarz[2], Ivan Gomez-Mestre[3], Ruth Meyer[2], Marie Domscheit[1], Fabian Bartels[1], Sarah-Maria Schaeffer[2], Karolin Engelkes[4,5]

[1]*Zoological Institute, Technische Universität Braunschweig, Mendelssohnstraße 4, 38106 Braunschweig, Germany*

[2]*Institute of Geosystems and Bioindication, Technische Universität Braunschweig, Langer Kamp 19c, 38106 Braunschweig, Germany*

[3]*Ecology, Evolution, and Development Group, Department Ecology and Evolution, Doñana Biological Station, CSIC, 41092 Seville, Spain*

[4]*Leibniz Institute for the Analysis of Biodiversity Change, Martin-Luther-King-Platz 3, 20146 Hamburg, Germany*

[5]*Institute of Evolutionary Biology and Ecology, University of Bonn, An der Immenburg 1,53121 Bonn, Germany*

Corresponding author: **Katharina Ruthsatz**; ORCID: 0000-0002-3273-2826. Current address: Zoological Institute, Technische Universität Braunschweig, Mendelssohnstraße 4, 38106 Braunschweig, Germany. Phone: 0049 531 3912393. Email: katharinaruthsatz@gmail.com.

Material and Methods

When supplying the particles to the water, we used the following procedure:

1. One liter of aged water was added to the aquarium.
2. Particles (MP or cellulose) were then added to the aquarium.
3. The aquarium was filled up to the target water level (i.e., 9 L).

This process resulted in uniform particle dispersion in the water. The uniform dispersion was maintained by the air-stones until the next water change.

Determination of particle count and density

We weighed 0.0030 g of polyethylene microplastic (MP) particles (Sigma-Aldrich, CAS number 9002-88-4, density 0.94 g/mL) (Sartorius GmbH Göttingen, A120S) directly onto a glass slide. Subsequently, portions of the particles were transferred to clean slides and dispersed in drops of glycerin (86 %; Carl Roth GmbH, article number 7533.4) using a preparation needle under a stereomicroscope (Type). The residual particles that remained on the original slide were also dispersed in glycerin and all resulting 12 slides were covered with a coverslip before being digitized (Olympus Slideview VS200, magnification: 10x, EFI-option). The residual particle on the needle were counted under the stereomicroscope (n=72).

The digital images of the slides were imported into Fiji (version 2.9.0, based in ImageJ version 1.53t; Schindelin et al., 2012; Schneider et al., 2012) using the plugin OlympusImageJPlugin (version 2.3.1; Evident Corporation); the image data were too large to be imported in the original resolution, therefore, the images were down sampled during import which resulted in a pixel size of 2.1903 µm. Images were prepared for automatic particle counting by conversion to 16-bit grey scale and threshold-based removal of the dark borders of the glycerin using the wand tool and enlarging the selection by 1 pixel. Subsequently, all parts of the image showing no glycerin (i.e., MP particles) or inhomogeneous background coloring (e.g., close to the border of the slide) were filled white. MP particles were counted by setting a threshold that selected the particles only, creating a mask, filling the holes in the mask, and running the watershed algorism on the mask-image to separate adjacent particles. The number of MP particles were then automatically counted using the function “Analyze particles…”; only those particles with a size larger than two pixels (i.e., > 4.38 µm) were considered.

The mask was used to select all counted MP particles in the original (down sampled) image and color those particles white to indicate that they were counted. Particles that were not counted by the automatic approach (i.e., in the regions filled white for the automatic counting) were counted manually.

In total 489,325 MP particles were counted this way (Table A; including the residual particles on the preparation needle).

Table A: Counts of MP particles per slide (0.0030 g of MP in total).

Slide-number	Number of MP particles counted automatically	Number of MP particles counted manually
0	68285	471
1	51584	641
2	65084	354
3	47391	221

4	35449	51
5	36514	62
6	32406	74
7	25134	107
8	28940	168
9	49077	105
10	17978	426
11	28704	27

A visual inspection of the results provided through the automatic particle counting revealed that, occasionally, adjacent particles were counted as one. To estimate the error, a region of 500x500 pixels was arbitrarily selected in each image. The number of particles in these images were automatically counted as above and, in addition, manually assessed. The actual count of MP particles might be slightly higher (1.0582 to 1.0908-fold, based on mean and median of estimate of error) than the automatically assessed count (Table B). We therefore estimated about 172,601.2 to 177,918.5 MP particles per 0.0010 g, which corresponds to 1.0356-1.0675 x 10^7 particles per liter in our experiment.

Table B: Results of automatic and manual counting the number of MP particles on sub-images of 500x500 pixels.

Slide-number	Number of MP particles (automatic count)	Number of MP particles (manual count)	Manually counted number divided by automatically counted number, estimate of error
0	165	159	0.9636
1	398	445	1.1181
2	250	276	1.1040
3	124	124	1.0000
4	101	89	0.8812
5	91	101	1.1099
6	55	61	1.1091
7	49	54	1.1020
8	50	53	1.0600
9	161	172	1.0683
10	113	122	1.0796
11	49	54	1.1020

References

Schindelin, J., Arganda-Carreras, I., Frise, E., Kaynig, V., Longair, M., Pietzsch, T., Preibisch, S., Rueden, C., Saalfeld, S., Schmid, B., Tinevez, J.-Y., White, D.J., Hartenstein, V., Eliceiri, K., Tomancak, P., Cardona, A., 2012. Fiji: an open-source platform for biological-image analysis. Nat Methods, 9(7), 676–682. https://doi.org/10.1038/nmeth.2019

Schneider, C.A., Rasband, W.S., Eliceiri, K.W., 2012. NIH Image to ImageJ: 25 years of image analysis. Nat Methods, 9(7), 671–675. https://doi.org/10.1038/nmeth.2089

Table S1. Definition of morphometric measurements acquired from twelve arbitrarily selected juvenile specimens per treatment; measured in dorsal view. The points for measurement acquisition were selected such that they were comparable, easy to identify across specimens, and allowed for taking measurements approximately parallel to the respective bones.

Morphometric measure	**Definition**
Length of forelimb	Distance from the dorsal midpoint of the skinfold marking the trunk-forelimb transition to the tip of the 3rd finger; measured with the following intermediate points: elbow, root of 3rd finger, joint between phalanges of 3rd finger
Femur	Distance between the dorsal midpoint of the skin fold marking the trunk-hindlimb transition and the most distal (i.e., outer) point of the skinfold at the knee.
Tibiofibula length	Distance between the most distal point of the skinfold at the knee and the most distal (i.e., ventral) point of the skinfold at the ankle
Foot length	Distance between the most distal point of the skinfold at the ankle and the tip of the 4th toe; measured as cumulated distance between several intermediate points to account for bended toes

Table S2. Mean (± SD) larval period (days after hatching), snout-vent length (SVL, mm), body mass (mg), growth rate (GR, mg/dah), body condition (SMI), standard metabolic rate (SMR, mL O_2/h/g), CORT level (pg/mg), body width (mm), hepatosomatic index (HSI), length of forelimb (LOF, mm), length of hindlimb (LOH, mm), tibiofibular length (TFL, mm), and femur length (FEM, mm). Larvae: Late larvae (i.e., developmental stage NF57(Nieuwkoop & Faber 1994). Juveniles: Completion of metamorphosis + 10 days. N is the total number of analyzed individual animals, and n is the total number of tested aquaria. NA = not applicable. See text for further details.

Life stage	Treatment	Rearing temperature (°C)	Larval period	SVL	Body mass	GR	SMI	SMR	CORT	Body width	HSI	LOF	LOH	TFL	FEM
Larvae	Control	25	25.07(±0.45)	15.50(±0.68)	507.93(±109.31)	19.42(±4.37)	360.21(±35.61)	0.017(±0.002)	14.92(±10.33)	NA	NA	NA	NA	NA	NA
		28	23.00(±0.37)	14.46(±0.58)	395.20(±95.13)	16.28(±4.26)	351.83(±51.72)	0.024(±0.004)	19.04(±20.85)	NA	NA	NA	NA	NA	NA
	MP	25	23.00(±0.53)	14.06(±0.65)	533.40(±95.64)	22.27(±4.16)	522.00(±44.55)	0.024(±0.005)	31.53(±11.16)	NA	NA	NA	NA	NA	NA
		28	19.00(±0.53)	13.03(±0.63)	394.80(±69.03)	19.65(±3.51)	495.56(±25.97)	0.034(±0.005)	24.75(±20.67)	NA	NA	NA	NA	NA	NA
	Cellulose	25	26.00(±0.37)	14.13(±0.58)	539.73(±139.41)	19.95(±5.38)	515.89(±78.29)	0.013(±0.002)	20.73(±9.62)	NA	NA	NA	NA	NA	NA
		28	23.07(±0.59)	12.90(±0.63)	405.07(±98.78)	16.61(±4.14)	521.97(±61.86)	0.024(±0.004)	21.79(±8.57)	NA	NA	NA	NA	NA	NA
Juveniles	Control	25	NA	19.67(±0.65)	944.67(±98.52)	NA	NA	NA	NA	7.33(±0.65)	2.11(±0.71)	10228.65(±1026.49)	30838.79(±2060.17)	8923.21(±562.16)	7735.00(±727.45)
		28	NA	17.17(±1.03)	625.25(±166.00)	NA	NA	NA	NA	6.33(±0.77)	2.02(±0.82)	9334.24(±769.23)	28163.65(±2349.03)	8066.41(±723.47)	7181.31(±669.89)
	MP	25	NA	20.50(±0.52)	1029.50(±131.132)	NA	NA	NA	NA	8.58(±0.90)	2.09(±0.49)	11066.59(±646.90)	33580.05(±985.88)	9700.45(±368.54)	8312.55(±372.09)
		28	NA	19.08(±1.67)	767.67(±161.82)	NA	NA	NA	NA	7.25(±0.86)	2.44(±0.76)	9388.24(±1162.29)	27948.66(±3265.28)	8182.19(±990.71)	7111.84(±793.66)
	Cellulose	25	NA	19.25(±0.62)	751.92(±71.54)	NA	NA	NA	NA	7.50(±0.52)	2.02(±0.76)	10024.71(±541.05)	30709.08(±836.07)	8897.16(±310.24)	7611.58(±259.66)
		28	NA	18.08(±0.99)	663.33(±80.64)	NA	NA	NA	NA	6.75(±0.86)	1.49(±0.74)	9696.41(±666.49)	29313.61(±1609.97)	8497.40(±414.05)	7486.12(±417.27)

Table S3. Spearman's rank correlation of dependent variables in late larvae at developmental stage NF57 (Nieuwkoop & Faber 1994). Larval period (days after hatching), snout-vent length (SVL, mm), body mass (mg), growth rate (GR, mg/dah), body condition (SMI), standard metabolic rate (SMR, mL O_2/h/g), and CORT level (pg/mg). N = 90; N=54 for CORT. Regular: Coefficient of correlation (ρ). Italic: P- values.

	Larval period	**SVL**	**Body mass**	**GR**	**SMI**	**SMR**	**CORT**
Larval period	-	0.488	0.379	-0.001	-0.071	-0.803	-0.073
SVL	*<0.001*	-	0.612	0.439	-0.386	-0.464	-0.196
Body mass	*<0.001*	*<0.001*	-	0.907	0.430	-0.347	-0.032
GR	*0.990*	***<0.001***	***<0.001***	-	0.508	-0.036	0.005
SMI	*0.506*	***<0.001***	***<0.001***	***<0.001***	-	0.066	0.226
SMR	***<0.001***	***<0.001***	***0.001***	*0.735*	*0.535*	-	0.108
CORT	*0.601*	*0.155*	*0.817*	*0.972*	*0.100*	*0.436*	-

Table S4. Spearman's rank correlation of dependent variables at the end of experimental phase 2 (i.e., juvenile froglets 10 ten days after completing metamorphosis). Snout-vent length (SVL, mm), relative body width (mm × SVL^{-1}), hepatosomatic index (HSI), length of forelimb (LOF, mm), length of hindlimb (LOH, mm), tibiofibular:femur ratio (TFF ratio). N = 72; N=36 for HSI. Regular: Coefficient of correlation (ρ). Italic: P- values.

	SVL	**Body mass**	**Relative Body width**	**HSI**	**Relative LOF**	**Relative LOH**	**TFF ratio**
SVL	-	0.780	0.524	0.335	0.077	-0.013	0.144
Body mass	*<0.001*	-	0.519	0.042	0.182	0.188	0.262
Relative body width	*<0.001*	*<0.001*	-	-0.047	0.029	0.360	-0.023
HSI	*0.046*	*0.806*	*0.788*	-	0.044	-0.184	0.112
Relative LOF	*0.520*	*0.126*	*0.811*	*0.798*	-	0.409	0.057
Relative LOH	*0.912*	*0.113*	*0.002*	*0.284*	*<0.001*	-	-0.162
TFF ratio	*0.229*	*0.026*	*0.845*	*0.514*	*0.635*	*0.174*	-

Table S5. Mean (±SD), minimum, and maximum values of absolute counted MP particles as well as the mean (±SD) number of MP particles × g^{-1} per treatment before and after metamorphosis in the African clawed frog (*X. laevis*). Accumulation of MP was assessed in late larvae (i.e., developmental stage NF57, Nieuwkoop & Faber 1994) and juveniles (i.e., 10 days after completing metamorphosis). One larva and four juveniles of each aquarium were randomly selected and analyzed, respectively. The larvae (N=18) and half of the juveniles (N=36) were processed and analyzed in total, whereas in the second half of the juveniles (N=36) the guts were dissected and analyzed individually. N(n) = total number of studied individuals (total number of aquaria). See text for further details.

Life stage	**Sample type**	**Temperature (°C)**	**Treatment**	**Absolute MP count mean (±SD)**	**Absolute MP count minimum**	**Absolute MP count maximum**	**Relative MP count (particles × g^{-1}) mean**
Larvae	whole-body	25	Control	0	0	0	0
			MP	63.66	49	142	177.83
			Cellulose	3	1	8	9.92
		28	Control	0	0	0	0
			MP	89.67	12	195	284.97
			Cellulose	2.66	0	8	7.94
Juveniles	whole-body	25	Control	0.5	0	3	0.65
			MP	17	0	97	16.53
			Cellulose	0.5	0	2	0.65
		28	Control	0.5	0	3	0.86
			MP	5.83	0	35	6.42
			Cellulose	0	0	0	0
	gut	25	Control	0.83	0	3	35.14
			MP	25	0	90	888.70
			Cellulose	0.5	0	2	22.42
		28	Control	0.33	0	2	47.61
			MP	15.16	0	87	521.29
			Cellulose	0	0	0	0
	body remnant	25	Control	0.5	0	2	0.52
			MP	0.66	0	2	0.70
			Cellulose	0	0	0	0
		28	Control	0.33	0	1	0.54
			MP	0.33	0	1	0.45
			Cellulose	1.16	0	6	1.89

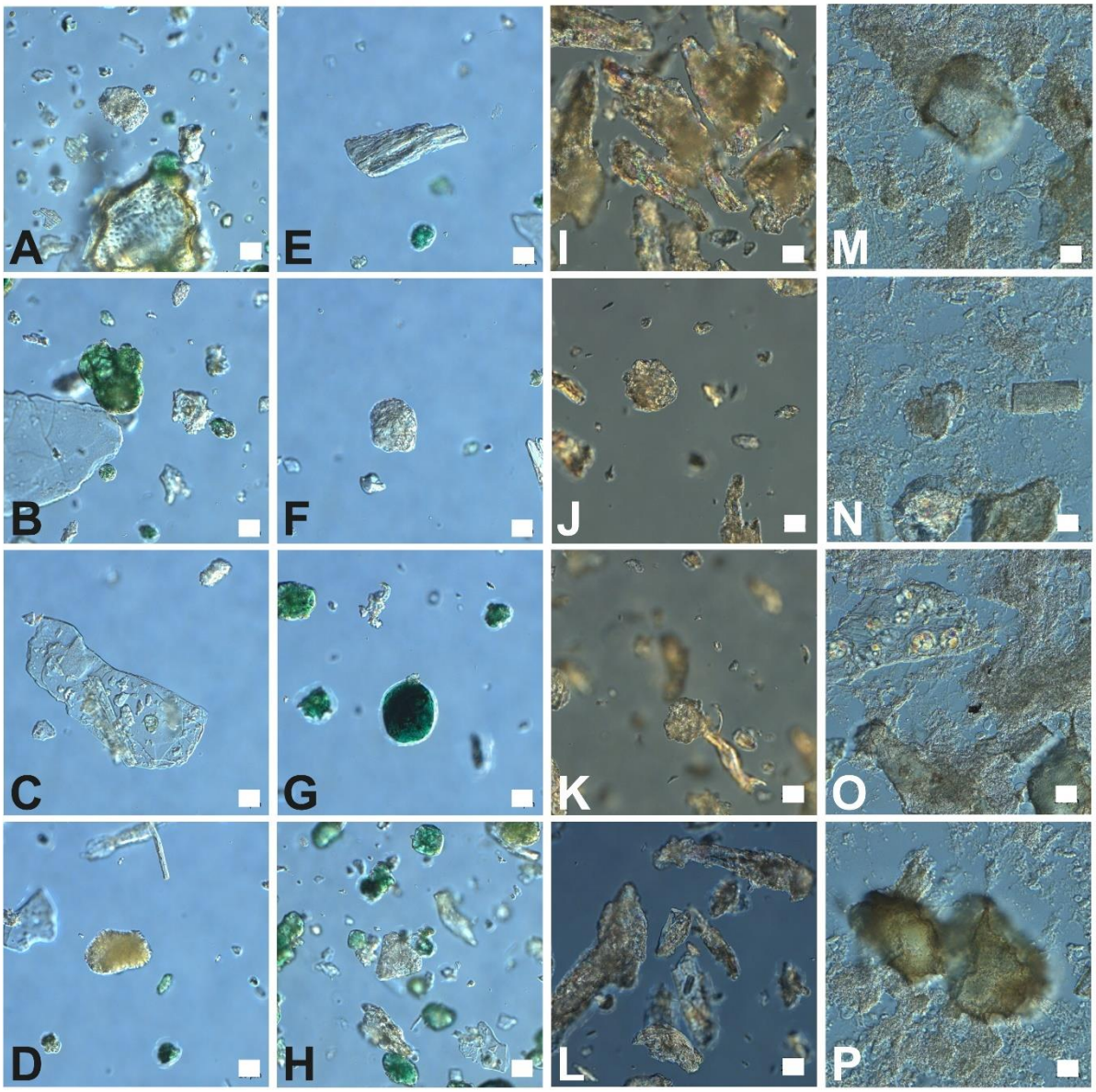

Fig. S1. Before the start of the experiment, both food types and the cellulose powder were checked for polyethylene MP particles used in the present study to control for contamination. **A-H** Larval food (Sera micron breeding feed for fish and amphibians, Sera, Germany). **I-L** Cellulose powder (Sigma-Aldrich; cellulose powder, CAS number 9004-34-6, particle size: 51 µm). **M-P** Juvenile food (Tetra ReptoFrog Granules for aquatic amphibians, Tetra GmbH, Germany). Even if some particles looked similar to the MP particles used in the present study (e.g., **A**, **F**, **J**, and **N**), we could not find any polyethylene MP particles in food samples of the larval food nor the juvenile food, or in the Cellulose powder. Particles similar to polyethylene MP were smaller, flatter, or had a different surface than the polyethylene MP particles used in the present study. Width of white rectangle: 20 µm. See text for further details.

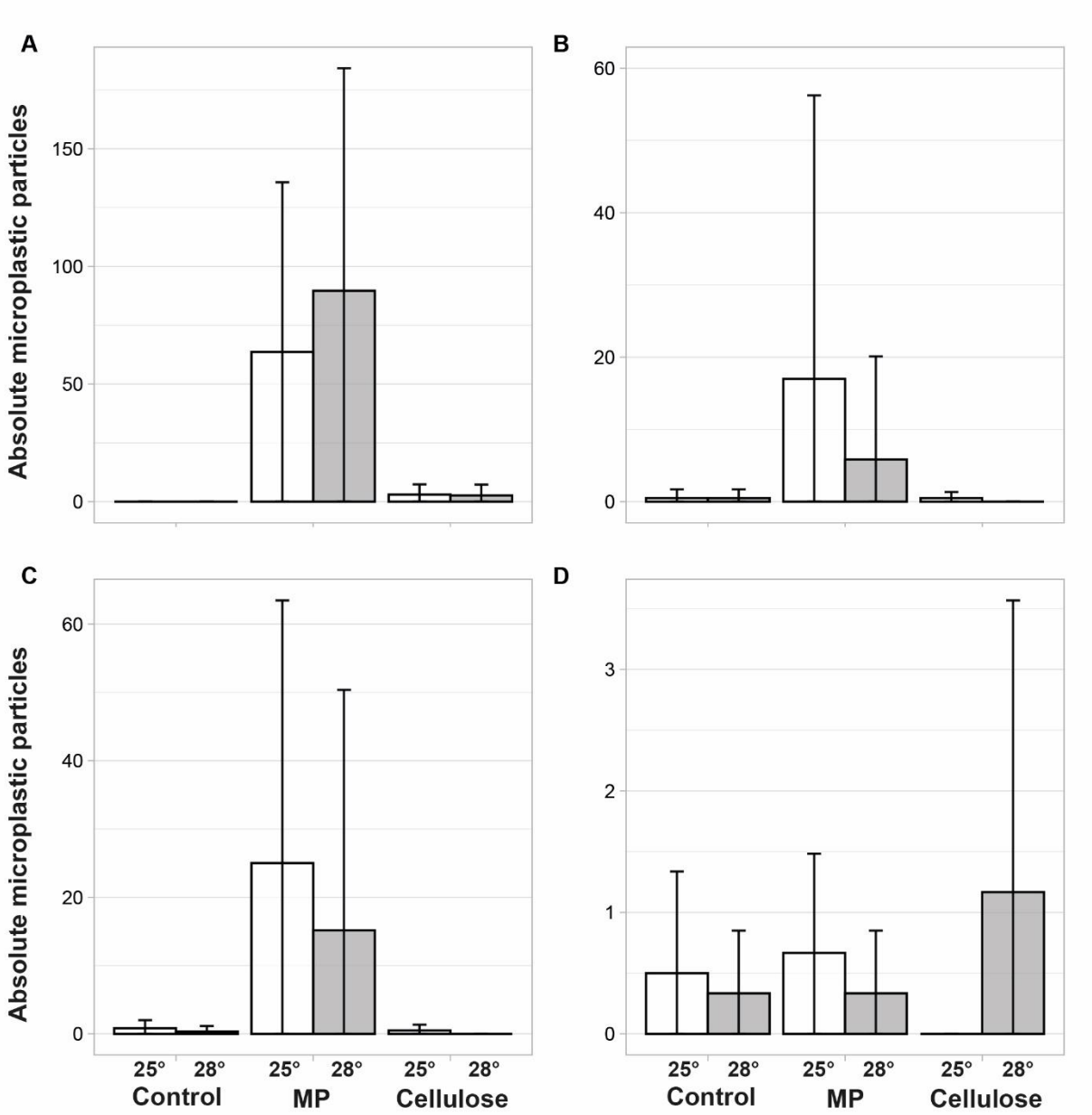

Fig. S2. Mean absolute number of MP particles (±SD) per treatment in late larvae (i.e., developmental stage NF57, Nieuwkoop and Faber, 1994) and in juveniles (i.e., ten days after completing metamorphosis at NF66, Nieuwkoop and Faber, 1994) in *Xenopus laevis*. One larva and four juveniles of each aquarium were randomly selected and analyzed, respectively. The larvae (**A**; N=18) and half of the juveniles (**B**; N=36) were processed and analyzed in total, whereas in the second half of the juveniles (N=36) the guts were dissected. Both the guts (**C**) and the body remnants (**D**) after gut dissection were analyzed individually.